Electrolyte materials and interfacial engineering for high-energy-density aqueous potassium-ion batteries

Changjian Li[#1], Xiaoyu Huo[#1], Jian Feng[1], Lai Wei[1], Kezhuo Li[1], Dongyang Shen[1], Kai Liu[1,2]✉

[1]Department of Chemical Engineering, Tsinghua University, Beijing 100084, China

[2]State Key Laboratory of Chemical Engineering and Low-Carbon Technology, Beijing 100084, China

Carbon Future 2026, 3, 9200087 https://doi.org/10.26599/CF.2026.9200087

Received: July 8, 2026; Revised: August 25, 2026; Accepted: September 3, 2026

# Changjian Li and Xiaoyu Huo contributed equally to this work

✉Address correspondence to Kai Liu, liukai2019@tsinghua.edu.cn

Abstract

Aqueous potassium-ion batteries (AKIBs) have emerged as highly attractive candidates for grid-scale energy storage due to their intrinsic safety, low cost, and fast ion transport kinetics. However, their practical deployment is severely impeded by insufficient energy density, typically falling below 80 Wh kg^{-1}, which is largely attributed to the narrow electrochemical stability window of conventional dilute electrolytes and subsequent electrode degradation. To address this critical bottleneck, this article provides a systematic overview dedicated to boosting the energy density of AKIBs. We comprehensively evaluate recent advances from two key dimensions: phase-transition mitigation and structural hydration engineering through water-in-salt electrolytes and hydrogen-bond regulation. Specifically, the evolution of electrolyte design from super-concentrated formulations to cost-effective fluorine-free alternatives and less salt hybrid concepts are elucidated. Finally, we outline persisting challenges and offer strategic outlooks regarding interfacial chemistry and realistic full-cell metrics to facilitate the practical development and commercialization of high-energy-density AKIBs.

Keywords: Aqueous Potassium-Ion Batteries, Energy Density, Water-in-Salt Electrolytes, Hydrogen-Bond Regulation, Electrochemical Stability Window

1 Introduction

The development of high-performance, cost-effective, and safe energy storage technologies is a crucial cornerstone for achieving global carbon neutrality goals.[1-17] Among various energy storage systems, conventional lithium-ion batteries employing nonaqueous electrolytes are increasingly constrained in grid-scale applications by inherent safety hazards, such as catastrophic fires or explosions, as well as rising cost and supply-chain concerns.[18-25] Consequently, aqueous rechargeable batteries have emerged as a highly attractive alternative due to their intrinsic safety, low cost, environmental sustainability, and high ionic conductivity. In particular, aqueous potassium-ion batteries (AKIBs) have garnered significant interest within both academic and industrial sectors.[26-31] This growing interest originates from both the natural abundance of potassium resources and the unique physicochemical properties of K^+. The relatively low redox potential of K^+/K (-2.93 V vs. standard hydrogen electrode [SHE]) enables AKIBs systems to deliver a competitive operating voltage. Furthermore, K^+ exhibits the smallest hydrated radius and the lowest hydration free energy despite its relatively large bare ionic radius. These characteristics facilitate rapid de-solvation and exceptionally fast ion transport kinetics, thereby endowing AKIBs with excellent rate capabilities.[32] As summarized in (Figure 1)[33-35], this review systematically discusses the major electrolyte engineering strategies developed for high-energy-density AKIBs.

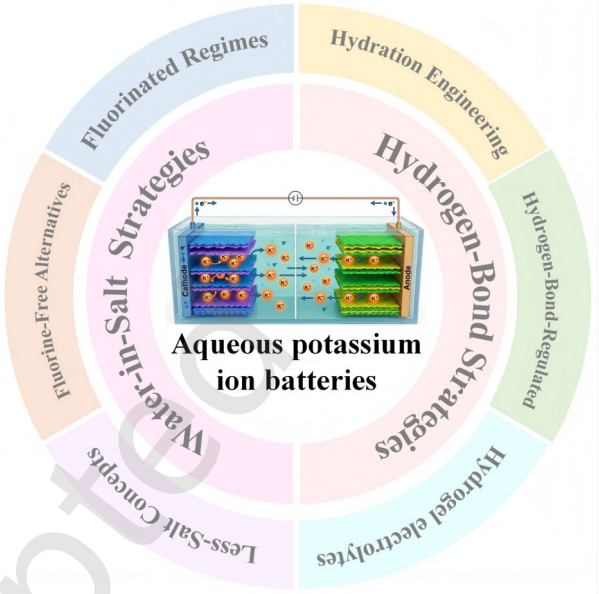

Figure 1. Schematic illustration of electrolyte engineering strategies for AKIBs. The diagram summarizes key approaches categorized into Water-in-Salt Strategies (Fluorinated Regimes, Fluorine-Free Alternatives, and Less Salt Concepts) and Hydrogen-Bond Strategies (Hydration Engineering, Hydrogen-Bond-Regulated, and Hydrogel electrolytes) to optimize battery performance.

Although Neff first demonstrated the electrochemical feasibility of Prussian Blue (PB) for AKIBs in 1978,[36] the field remained largely unexplored for several decades before experiencing rapid growth in recent years. (Figure 2)[37-39] Prior to 2020, research endeavors in AKIBs were predominantly dedicated to identifying viable electrode materials, ranging from Prussian blue analogues and intercalation pseudocapacitive oxides to electroactive organic polymers. While these pioneering works successfully broadened the portfolio of electrode materials, the narrow electrochemical stability window of dilute aqueous electrolytes severely restricted the cell voltage and cycling stability. (Figure 2)[31] Despite these promising attributes,

the practical deployment of AKIBs is severely impeded by their **insufficient energy density**, with most full-cell configurations delivering below 80 Wh kg^{-1}. From a materials perspective, representative K-storage electrodes can be grouped into layered transition-metal oxides, Prussian blue analogues (PBAs), polyanionic compounds, and organic compounds. Layered oxides can offer high capacity and tunable redox chemistry but may undergo K^+/H^+ exchange, air-induced degradation, and phase transitions. PBAs provide open three-dimensional diffusion channels and low-strain K^+ insertion, whereas vacancies, coordinated water, Jahn–Teller distortion, and transition-metal dissolution can compromise durability.[40, 41] Polyanionic compounds generally possess robust frameworks and high redox potentials, but their limited electronic conductivity often requires conductive-network engineering and their gravimetric capacities can be modest. Organic compounds offer molecularly programmable redox sites and potentially favorable low-temperature kinetics, but dissolution and low-potential water reduction frequently necessitate electrolyte-derived passivation. These material-specific failure modes determine the required electrolyte window and interfacial chemistry.[42-45] Thermodynamically, the energy density of a battery system is fundamentally governed by the cell operating voltage and the specific capacity of the electrode materials. The primary bottleneck restricting the energy density of AKIBs stems from the narrow electrochemical stability window (ESW) of traditional dilute aqueous electrolytes, which is intrinsically limited to a mere 1.23 V by the high activity of water. When the operating voltage exceeds this thermodynamic limit, the parasitic hydrogen evolution reaction (HER) at the anode and the oxygen evolution reaction (OER) at the cathode inevitably occur. These irreversible water decomposition side reactions not only trigger severe active material dissolution and rapid capacity decay, but also compromise coulombic efficiency and induce significant concentration polarization. More critically, the continuous generation of gaseous byproducts (H_2 and O_2) elevates internal cell pressure,[46] potentially causing cell swelling, leakage, and safety hazards. Consequently, **expanding the ESW by suppressing water decomposition has become a key objective in AKIBs research**.[47] Recent nonaqueous potassium-ion battery studies further demonstrate that electrolyte and electrode design are inseparable. Methyl-asymmetry-regulated electrolytes have improved high-voltage compatibility with graphite by reducing K^+ desolvation barriers and promoting inorganic interphase formation, whereas interfacial-electric-field engineering of $KVPO_4F$ has stabilized a thin cathode–electrolyte interphase and high-voltage cycling. Broader built-in-electric-field frameworks likewise connect electrode electronic structure with selective charge transfer and interphase formation. These studies are cited here as transferable design principles rather than direct AKIB demonstrations.

While substantial efforts have been devoted to electrode engineering, recent research has increasingly focused on electrolyte solvation structure modulation as a more effective route for overcoming the intrinsic voltage limitation of aqueous systems. A milestone breakthrough in this domain was the introduction of highly concentrated "water-in-salt" electrolytes (Figure 2). Throughout this review, lowercase m denotes molality (mol kg^{-1} of solvent; H_2O for purely aqueous electrolytes unless otherwise specified), whereas uppercase M denotes molarity (mol L^{-1} of solution). These two concentration scales are not interconverted without density data. By dramatically increasing the salt molality toward

its solubility limit (e.g. 22 M KOTf or 30 M KFSI), the salt-to-water ratio undergoes a profound inversion. Consequently, the vast majority of water molecules are tightly locked within the primary solvation sheath of K^+, minimizing the population of uncoordinated "free water" clusters. This unique solvation restructuring significantly reduces water activity by disrupting the hydrogen-bond network and decreasing the population of free water molecules. Moreover, the participation of anions in the primary solvation sheath promotes preferential anion reduction at the electrode surface, leading to the formation of robust anion-derived interphases.[48] These interphases effectively passivate the electrode surface against water infiltration, offering kinetic stability that expands the ESW up to 3-4 V.[31, 49, 50]

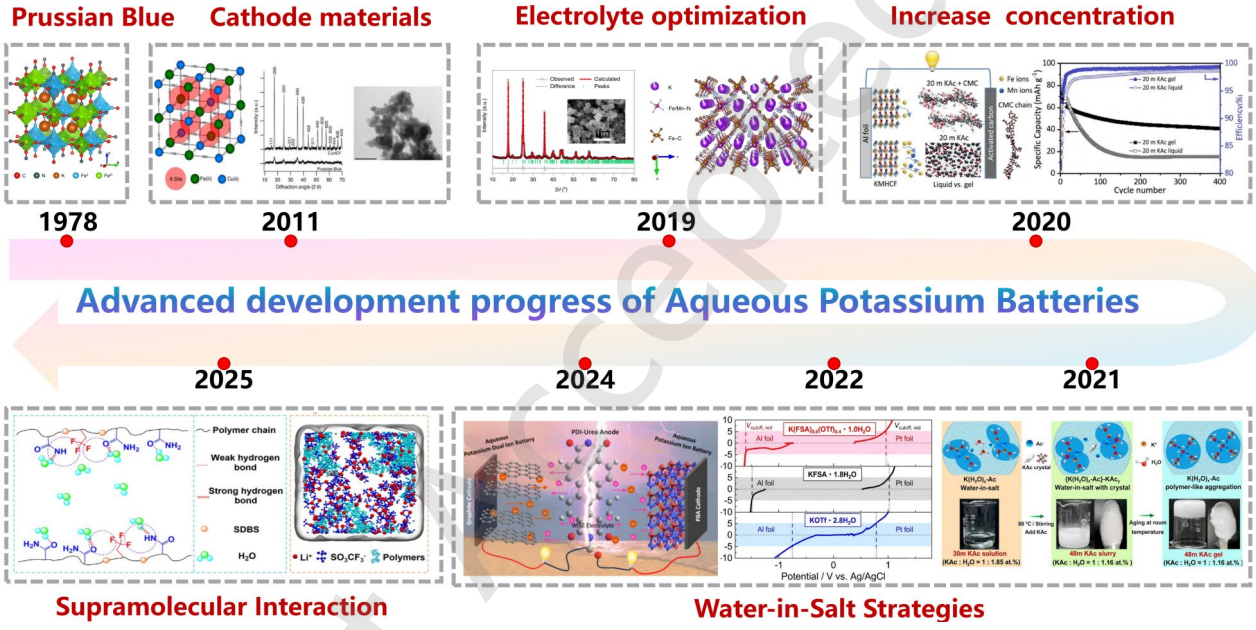

Figure 2. The advanced development progress of aqueous potassium batteries. The roadmap highlights critical milestones from early **Cathode materials** exploration (Prussian Blue analogues since 1978 and 2011) to key electrolyte innovations, including **Electrolyte optimization** (2019), **Increase concentration** (2020), **Water-in-Salt strategies** (2021-2024), and recent emerging **Supramolecular interaction** networks (2025). Ref. [36] ©1978 The Electrochemical Society; Ref. [31] © 2019, Springer Nature; Ref. [34] © 2020 Elsevier Ins.; Ref. [51] © 2021 Elsevier Inc; Ref. [49] ©2022 Elsevier Inc.; Ref. [50] © 2024 American Chemical Society; Ref. [52] © 2025 Elsevier Inc.

Nevertheless, the pursuit of ultra-high salt concentrations inevitably introduces several practical drawbacks, including high costs of fluorinated imide salts, increased electrolyte viscosity, diminished ionic conductivity, and a propensity for salt precipitation under low-temperature conditions. To achieve ESW expansion without relying exclusively on extremely high salt concentrations, **hydrogen-bond regulated electrolytes** have emerged as an elegant and cost-effective alternative. (Figure 2) The thermodynamic and kinetic processes governing water electrolysis are closely related to the dynamics of the hydrogen-bond network of

free water molecules. By introducing electrochemically inert, highly polar organic co-solvents or supramolecular hosts (e.g., succinonitrile [SCN], trimethyl phosphate [TMP], or (2-hydroxypropyl)-β-cyclodextrin [HBCD]), the intrinsic tetrahedral hydrogen-bonding framework of water can be selectively disrupted at the molecular scale.[52, 53] These functional co-solvents either directly participate in the K^+ coordination shell to displace water molecules or sequester water into confined spaces via hydrogen-bonding networks and excluded-volume effects. Through simultaneous thermodynamic suppression of water activity and kinetic restriction of water accessibility at electrode interfaces highly reactive free water molecules are transformed into less reactive bound-water states. As a result, electrochemical stability windows approaching or even exceeding 4 V can be achieved at relatively low salt concentrations. Consequently, hydrogen-bond regulation offers a powerful design paradigm that balances energy density, cost-effectiveness, and transport kinetics.[54]

Given these critical developments, this review provides a focused and systematic overview dedicated to enhancing the energy density of AKIBs. We summarize and critically discuss the recent progress in widening the ESW through two pivotal strategies: solvation-structure engineering based on **concentrated electrolytes (WiSE)** and **hydrogen-bond network regulation**. Particular emphasis is placed on the evolution of concentrated electrolyte design, from superconcentration regimes, transitioning toward eco-friendly fluorine-free alternatives for cost reduction, and emerging less-salt approaches that retain favorable "WiSE" nature while reducing salt consumption. Furthermore, we discussed how functional co-solvents reconstruct micro-scale hydrogen-bonding environments to deactivate free water molecules and enhance overall full-cell electrochemical metrics. Compared with previous reviews that broadly catalogue electrode chemistries or aqueous potassium storage, this Review makes three key contributions. First, it establishes a hierarchical framework linking concentration-induced K^+ solvation reconstruction with hydrogen-bond and water-state regulation. Second, it systematically summarizes two major electrolyte strategies for enhancing the energy density and performance of AKIBs: water-in-salt electrolytes and hydrogen-bond regulation. Third, by comparing their effects on solvation structures, it reveals the intrinsic relationship between water activity and K^+ storage behavior, clarifying the mechanisms of side-reaction suppression and electrochemical-window expansion and providing guidance for high-performance AKIB electrolyte design. Finally, the persistent challenges of these electrolyte modulation strategies and future insights are highlighted to facilitate the practical implementation and industrial deployment of high-energy-density AKIBs.

2 The Evolution of "Water-in-Salt" Strategies: From Superconcentration Regimes to Cost-Effective and Less-Salt Paradigms

In conventional low-concentration Salt in Water (SIW) electrolytes, the system is dominated by abundant free water molecules, where cations are encapsulated by well-defined primary and secondary hydration sheaths while anions remain fully dissociated. Upon migrating to the ultra-high-concentration WiSE regime, the severe scarcity of solvent molecules triggers a profound reconstruction of the local coordination environment.[55-58] Due to the deficit of available water molecules within the co-sphere, anions are energetically forced to enter the primary solvation sheath of cations. This structural transition from a purely aqueous coordination to an anion-water co-controlled configuration

effectively tethers the remaining water molecules via intense electrostatic interactions, thereby drastically suppressing their thermodynamic activity and inherently expanding the electrochemical stability window of aqueous electrolytes.(Figure 3)

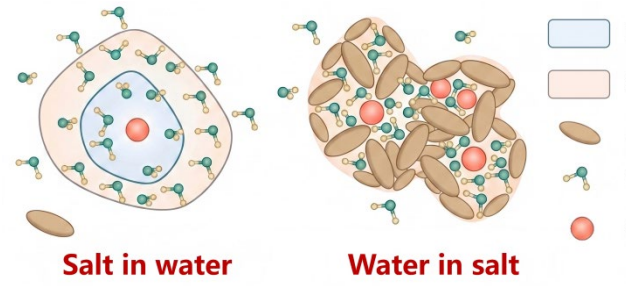

Figure 3. The evolution of cation solvation structure with increasing salt **concentrations.**

2.1 Fluorinated Regimes: Pursuing Ultimate Voltage Windows

Fluorinated regimes have emerged as a key strategy for expanding the electrochemical stability window and enabling higher operating voltages in advanced energy storage systems. Liang et al. reconstructed commercial orthorhombic V_2O_5 into δ-$K_{0.5}V_2O_5$(KVO) nanobelts with an enlarged interlayer spacing and anisotropic ion-transport pathways for aqueous K-ion batteries. (in Figure 4a)[58] The as-prepared KVO cathode delivered a high capacity of 116 mA h g^{-1} at 1 C and retained 65 mA h g^{-1} at 50 C, together with 88.2% capacity retention after 1000 cycles at 1 C. When paired with a PTCDI anode in a full-cell configuration using a 22 m KCF_3SO_3 water-in-salt electrolyte, the device achieved 77.3% capacity retention over 20,000 cycles at 10 C and exhibited satisfactory operation at -30°C. Density functional theory (DFT) calculations and experimental results revealed that the superior rate capability originated from the low-energy-barrier K^+ diffusion and enhanced electronic conductivity, while the water-in-salt electrolyte effectively suppressed vanadium dissolution and stabilized the reversible phase transition during potassiation/depotassiation.

Hosaka et al. have made notable contributions to the development of advanced aqueous electrolyte systems aimed at expanding electrochemical stability windows and improving cycle durability in aqueous alkali-ion batteries. Initially, they developed a monohydrate-melt electrolyte for AKIBs by forming a eutectic mixture of potassium bis(fluorosulfonyl)amide and potassium triflate in a 6:4 molar ratio. (in Figure 4b)[49] They demonstrated that this $K(FSI)_{0.6}(OTf)_{0.4}\cdot 1.0H_2O$ electrolyte exhibited a wider electrochemical potential window of 2.56 V compared to the individual salt hydrates. Furthermore, they showed that this hydrate-melt significantly improved the cycle life of full cells based on a PTCDI anode and a $K_2Fe_{0.5}Mn_{0.5}[Fe(CN)_6]$ cathode. Their investigation revealed that the capacity retention was enhanced because the monohydrate-melt minimized the degradation of both the electrode morphology and the crystal structure of the Prussian blue analogue cathode. Additionally, they found that PTCDI remained insoluble in the hydrate-melt and reversibly stored K^+, facilitated by the formation of a solid electrolyte interphase composed of decomposed FSI^- products like KF. Building on this concept, they further developed a superconcentrated aqueous electrolyte system based on a eutectic NaFSI-KFSI composition via a synergistic Na^+/K^+ dual-cation strategy.[17] Experimental results showed that 35 m $Na_{0.55}K_{0.45}FSI/H_2O$ and 33 m $Na_{0.45}K_{0.55}FSI/H_2O$ solutions could be formulated at 25°C. Compared with saturated single-cation NaFSI or KFSI solutions, the mixed electrolytes delivered a much wider electrochemical potential window of ~3.5 V. When applied to two battery configurations such as carbon-coated $Na_2Ti_2(PO_4)_3|K_2Mn[Fe(CN)_6]$ and $Na_3V_2(PO_4)_3|K_2Mn[Fe(CN)_6]$, the former

exhibited highly reversible charge-discharge profiles with a mean discharge voltage of 1.4 V, while the latter demonstrated 2 V operation despite slight capacity degradation. Mechanistic investigations revealed that a Na-rich solid electrolyte interphase dominated by NaF formed on the anode surface, and the anode and cathode primarily accommodated Na^+ insertion and co-insertion of Na^+ and K^+, respectively, confirming the feasibility of this dual-ion aqueous battery system. (in Figure 4c)

Later, the same group employed in situ scanning electrochemical microscopy (SECM) and operando electrochemical mass spectrometry (OEMS) to elucidate the properties of the solid electrolyte interphase (SEI) formed in a 55 m $K(FSI)_{0.6}(OTf)_{0.4}$ highly concentrated WiSE, using a 3,4,9,10-perylenetetracarboxylic diimide (PTCDI) anode as a model system.[31] For the first time, passivating SEI structures with slow apparent electron transfer rates analogous to those in lithium-ion batteries were identified in the WiSE system. SECM analysis revealed that the SEI formed stably at PTCDI potentials around -1.3 V vs. Ag/AgCl prior to detectable hydrogen evolution, yet exhibited heterogeneous, incomplete surface coverage with exposed reactive regions remaining after 10 cycles. Complementary OEMS measurements demonstrated that the concentrated electrolyte shifted the onset of detectable H_2 evolution from -0.9 V in dilute analogues to below -1.4 V, enabling full access to PTCDI's two reversible redox processes, though the SEI failed to suppress H_2 evolution at more extreme negative potentials beyond -1.4 V. These findings highlighted both the passivating functionality of WiSE-derived SEI and its current limitations in covering electrode surfaces and expanding the electrolyte stability window, providing critical guidance for the rational design of high-performance aqueous batteries.

These critical findings on interfacial heterogeneity and the -1.4 V potential bottleneck underscore that relying solely on electrolyte concentration is insufficient. Instead, a holistic optimization encompassing both the cathode host lattice and the electrolyte environment is required to fully exploit the operating window. To bridge the gap between microscopic SEI limitations and macroscopic device longevity, recent breakthroughs have successfully integrated substitution strategies at the cathode with high-concentration regimes to stabilize the overall full-cell configuration. A prominent example is that Jiang et al. constructed a full aqueous AKIB based on a Fe-substituted Mn-rich Prussian blue analogue cathode, a 3,4,9,10-perylenetetracarboxylic diimide anode, and a 22 m KCF_3SO_3 WiSE.[31] They demonstrated that Fe substitution mitigated phase transitions and improved structural stability, enabling the optimized KFeMnHCF-3565 cathode to deliver a high capacity of approximately 135 mAh g^{-1}at 0.5 C, retain about 70% capacity at 100 C, and maintain 90% capacity retention over 10,000 cycles. Meanwhile, the highly concentrated electrolyte suppressed electrode dissolution due to the lack of free water and provided a wide electrochemical stability window. Benefiting from the synergistic effects of the cathode, anode, and electrolyte, the assembled AKIB operated stably in the range of 0-2.6 V, achieved a high energy density of 80 Wh kg^{-1}, exhibited excellent rate capability from 0.1 to 20 C, and retained 73% capacity after 2,000 cycles at 4 C. Furthermore, an 11 mAh pouch cell delivered good performance at low rates and over a broad temperature range from -20 to 60 °C, highlighting the promise of AKIBs for large-scale energy storage applications.

Beyond optimizing solvation kinetics via an individual fluorinated imide salt, expanding the chemical boundary of WiSEs has further inspired

the deployment of mixed-anion configurations within a quasi-solid-state matrix. By coupling the distinct passivation and coordination advantages of dual-salt components with the mechanical support of a hydrogel framework, researchers have successfully bypassed the fluidity limitations of conventional aqueous systems while maintaining excellent ion transport. A remarkable demonstration of this strategy from Li et al. addressed the long-standing trade-off between electrochemical stability and leakage risk of conventional aqueous electrolytes.(in Figure 4d)[59] The as-prepared WiSE, formulated with 20 m KCF_3SO_3 and 30 m KFSI, delivered an expanded electrochemical stability window of 3.02 V, outperforming its liquid water-in-salt electrolyte counterpart, alongside a high ionic conductivity of 4.34 mS cm^{-1} and excellent mechanical stretchability.(in Figure 4d) When paired with a $KMnFe(CN)_6$ cathode and nanostructured carbon-coated $KTi_2(PO_4)_3$ anode, the assembled full aqueous potassium-ion battery operated at a high voltage of 2.8 V, achieving a near-theoretical anode capacity of 135 mAh g^{-1} and remarkable cycling stability with 87.5% capacity retention after 3000 cycles, as well as good rate performance. This work provided a feasible strategy for designing safe, high-energy-density aqueous energy storage devices.

Kumaresan et al. introduced an asymmetric potassium imide salt, KCTFSI, containing cyano (C≡N) and trifluoromethanesulfonyl (TFSI) moieties, and demonstrated that structural asymmetry dramatically enhanced the solubility of potassium salts in water.[60] The electrolyte achieved an unprecedented concentration of 32.2 m, far exceeding that of symmetric KTFSI (1.5 m), owing to preferential C≡N–K^+ coordination and extensive contact-ion-pair formation. The resulting WiSE exhibited a widened electrochemical stability window of up to 3.80 V and remarkable supercooling behavior, remaining liquid at −15 °C for over one month. Full cells employing PTCDI anodes and $KVPO_4F$ cathodes delivered stable cycling with an average discharge voltage of 1.7 V even at −15 °C, highlighting asymmetric coordination engineering as an effective strategy to overcome the conventional requirement for extremely high-salt concentrations in aqueous potassium-ion batteries.

Chen et al. developed a KFSI-based aqueous WiSE to suppress organic-electrode dissolution and the hydrogen evolution reaction.[35] It is found that the 30 M high-concentration KFSI electrolyte drastically reduced the content of free water molecules, expanding the electrochemical stability window to 3.97 V, while effectively suppressing the dissolution of potassiated β-perylene-3,4,9,10-tetracarboxylic dianhydride (β-PTCDA) in the aqueous electrolyte. In addition, the electrolyte facilitated the dissociation of the K^+ solvation sheath, lowered reaction and charge transfer resistance, and significantly improved the potassium storage kinetics. The β-PTCDA anode based on this electrolyte delivered a stable specific capacity of 130 mAh g^{-1} at a current density of 0.2 A g^{-1}, retained 83% of its capacity at a high rate of 8 A g^{-1}, and maintained a capacity retention of 82% after 500 cycles at 2 A g^{-1}. The full cell assembled with a potassium iron(II) hexacyanoferrate (KFHCF) cathode exhibited excellent rate performance and long-term cycling stability, with a capacity retention of 89% after 1000 cycles at 12.5 C, and a maximum energy density of 41 Wh kg^{-1}, demonstrating promising application potential in medium- and large-scale energy storage.(in Figure 4e)

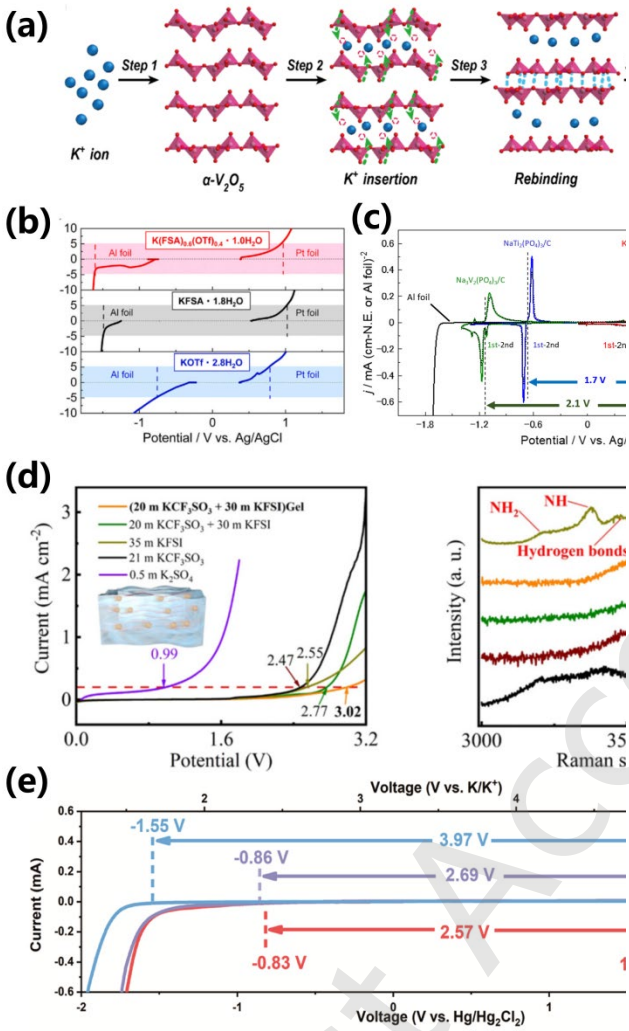

Figure 4. (a) Structural evolution of the reconstructing process from α-V_2O_5 to δ-KVO; (b) LSV curves of Al foil (cathodic scan) and Pt foil (anodic scan) working electrodes in $K(FSI)_{0.6}(OTf)_{0.4} \cdot 1.0H_2O$ (top), $KFSI \cdot 1.8H_2O$ (middle), and $KOTf \cdot 2.8H_2O$ (bottom) electrolytes. The potential window is defined by the difference in the potential reached at a current density of ±5 μA cm^{-2}; (c) Cyclic voltammograms of the positive (KMnHCF) and negative (NTP-C and NVP-C) electrodes in 33 M $Na_{0.45}K_{0.55}FSI$ solution at a scan rate of 0.1 mV S^{-1}. The LSV curves of Ti and Al foil for the respective anodic and cathodic scans are also shown; (d) The electrochemical stability window of each electrolyte was measured by LSV between 0 V and 3.2 V by using a Ti//Ti two-electrode system at a scan rate of 10 mV s^{-1} and inset is the structural architecture of the water-in-salt hydrogel electrolyte.(left); The Raman spectra of 1 m, 21 m KCF_3SO_3, 35 m KFSI, (20+30) m WIS, and (20+30) m K-ion water-in-salt hydrogel electrolyte in the range of 3000–4000 cm^{-1}.(right); (e) Linear voltammetry curves recorded at 10 mV s^{-1} in 1, 10, and 30 m KFSI electrolyte for a conventional β-PTCDA||KFHCF AKIB system. Reproduced with permission from Ref. [58] © 2021 American Chemical Society; Ref. [49] © 2022 Elsevier B.V.; Ref. [17] © 2022 American Chemical Society; Ref. [59] © 2021 Wiley-VCH GmbH; Ref. [35] © 2020 The Royal Society of Chemistry.

Vardhini et al. developed a perylene diimide-based anode (PDI-Urea) for aqueous potassium energy storage systems and systematically evaluated its electrochemical performance in three concentrated WiSE: 30 M potassium acetate, 40 M potassium formate, and 30 M potassium bis(fluorosulfonyl)imide (KFSI).[50] They identified 30 M KFSI as the optimal electrolyte due to its superior ionic conductivity (24 mS cm^{-1}), low internal resistance, and wide electrochemical stability window. The authors assembled an aqueous potassium dual-ion battery (APDIB) with a graphite cathode and a full aqueous K-ion battery (AKIB) with a Prussian blue analogue (PBA) cathode. The PDI-Urea//PBA AKIB exhibited excellent rate capability and outstanding cycling stability, retaining 91% of its capacity after 1000 cycles at 2 A g^{-1}. Ex-situ characterizations revealed that the charge storage relied on the reversible potassiation/depotassiation of urea carbonyl groups and the intercalation/deintercalation of FSI^- anions in graphite. Overall, the study demonstrated that combining organic polyimide anodes with KFSI-based WiSE effectively suppressed active material dissolution and enabled high-performance, sustainable aqueous potassium-ion energy storage.

2.2 Fluorine-Free Alternatives: Balancing Economic Sustainability and Alkaline Corrosion

Despite the advantages of fluorinated regimes in extending voltage windows, growing concerns over cost and sustainability have shifted attention toward fluorine-free alternatives that balance economic viability with alkaline corrosion resistance. Mona et al. systematically investigated the electrochemical charge storage properties of six porous carbons with distinct textural features in potassium acetate (KOAc) electrolytes spanning from dilute salt-in-water (1 m) to water-in-salt (27 m) concentrations.[56] It was demonstrated that the specific capacitance exhibited a positive correlation with both the total and micropore volumes of the carbons, with the contribution of micropores being more dominant. While the 27 m KOAc electrolyte enabled a maximum operational potential window of 1.4 V for porous carbon composite electrodes, the electrochemical stability window of all tested carbons showed negligible variation with increasing salt concentration, a trend that diverged from observations on ordered carbon electrodes such as glassy carbon. For the highly concentrated 27 m KOAc system containing bulkier ionic species, a limited mesopore volume was found to impair the rate capability of the electrodes. Notably, pseudocapacitive hydrogen sorption/desorption processes contributed to the charge storage at negative potentials, yet the hydrogen evolution reaction displayed no significant dependence on KOAc concentration when analyzed at a constant overpotential, despite the marked reduction in free water content in the 27 m electrolyte.

Beyond the fundamental charge storage behavior of porous carbons in concentrated acetate electrolytes, further efforts have focused on engineering the electrolyte structure to improve interfacial stability and enable practical potassium-ion storage. The study from the Jin group developed a fluorine-free, low-cost potassium acetate (KOAc)-based WiSE for aqueous potassium-ion batteries, where combined Raman spectroscopy and molecular dynamics (MD) simulations revealed that water was effectively coordinated by both acetate anions and potassium cations, yielding a sponge-like molecular arrangement akin to ionic liquids and significantly suppressed water activity.[34] Electrochemical characterization paired with SEM/EDX analysis demonstrated that a 20 m KOAc formulation optimally balanced aluminum current collector stability by preserving the native Al_2O_3 passivation layer, avoiding the severe corrosion observed in lower-concentration electrolytes and pitting induced by the excessive alkalinity of 30 m solutions. When paired with potassium manganese hexacyanoferrate (KMHCF) cathodes, the 20 m electrolyte delivered improved capacity and reversibility over more dilute counterparts, yet the alkaline environment still triggered active material degradation and metal dissolution, as confirmed by XPS and separator analysis. To address this limitation, a gelified electrolyte was fabricated by introducing 2 wt% carboxymethyl cellulose (CMC) into the 20 m KOAc system, which further reduced water mobility, lowered the system pH, and suppressed Mn/Fe leaching, ultimately enabling a stable discharge capacity of 41 mAh g^{-1} with a Coulombic efficiency exceeding 99.3% over 400 cycles, while offering a cost nearly three orders of magnitude lower than conventional fluorinated LiTFSI-based WiSE, highlighting its promise for large-scale stationary energy storage.

While liquid concentrated acetate based WiSEs have demonstrated improved stability and reduced water activity, further enhancement of interfacial stability and suppression of parasitic

reactions have motivated the transition toward quasi-solid or gelled electrolyte architectures. Liu et al. developed a polymer-free CH_3COOK gel electrolyte with an ultrahigh salt-to-water mole ratio of approximately 1:1.16, which exhibited an electrochemical stability window of 4 V versus Ag/AgCl.[51] They characterized the gel using Raman spectroscopy and density functional theory computations, revealing that nearly all free water molecules were eliminated and a cross-linked structure formed among K^+, CH_3COO^-, and H_2O . The authors reported that this electrolyte maintained a quasi-solid state over a broad temperature range from −20 to 90 °C, retaining considerable ionic conductivity alongside improved anti-deliquescence. When evaluated with a $FeSe_2$ anode in aqueous potassium-ion batteries, the gel electrolyte delivered a stable reversible capacity of about 250 mAh g^{-1} at 0.5 A g^{-1} and approximately 220 mAh g^{-1} at 1 A g^{-1} over 250 cycles. They concluded that the quasi-solid nature of the electrolyte effectively suppressed the solvent power of water and inhibited the dissolution of active materials, while a stable solid electrolyte interphase formed on the electrode surface further enhanced cycling stability. (in Figure 5a)

Building on the above advances, researchers have further extended the development of aqueous electrolytes toward more highly concentrated and structurally regulated systems to achieve superior stability and multifunctionality. A new study proposed a novel, eco-friendly and cost-effective WiSE based on highly concentrated 40 M potassium formate, where the water-to-salt molar ratio dropped to 1.38:1 with nearly no free water molecules remaining. (in Figure 5b)[61] Electrochemical tests demonstrated that the electrolyte delivered an ultra-wide potential window of up to 4 V (-2.5 to 1.5 V vs. Ag/AgCl) on a glassy carbon electrode, outperforming the previously reported concentrated potassium acetate (CH_3COOK) system with a more negative stable potential and higher ionic conductivity (46 mS cm^{-1} even at 40 M, exceeding that of fluorinated imide-based water-in-salt electrolytes and conventional organic lithium battery electrolytes). When paired with an activated carbon-based supercapacitive electrode, the system achieved a low discharge potential of -2.4 V vs. Ag/AgCl, alongside a high specific capacitance of 321 F g^{-1} at 5 A g^{-1} and 121 F g^{-1} retained at 20 A g^{-1}, indicating excellent rate performance. Additionally, the electrolyte enabled typical potassium-ion battery behavior for a $KTi_2(PO_4)_3$ (KTP) anode, delivering a reversible capacity of ~15 mAh g^{-1} at 0.1 A g^{-1}, proving its applicability for both aqueous supercapacitors and potassium-ion batteries.

Leonard et al. developed a low-cost, non-toxic potassium acetate (KOAc)-based WiSE for aqueous potassium-ion batteries.[55] By employing aluminum and titanium as the negative and positive current collectors, respectively, they demonstrated that a 30 m KOAc electrolyte exhibited a wide electrochemical stability window of 3.2 V (vs Ag/AgCl). When paired with a KTP anode, the KOAc-WiSE system enabled reversible K^+ storage, delivering a specific capacity of 53 mAh g^{-1}. The KTP electrode in this aqueous system showed superior kinetics and rate performance compared to its non-aqueous counterpart, along with excellent long-term cycling stability. This work highlighted the feasibility of using affordable, fluorine-free WiSE to expand the operational voltage window and improve the energy efficiency of AKIBs for large-scale energy storage applications.

The study from Iamprasertkun et al. pioneered the use of highly concentrated aqueous potassium fluoride (KF) as a low-cost, low-toxicity WiSE, employing basal plane highly ordered pyrolytic

graphite (HOPG) as a model carbon system to elucidate its electrochemical properties.[62] The 17 m KF electrolyte delivered an exceptionally wide potential window of up to 2.6 V, a significant expansion beyond the conventional thermodynamic limit of aqueous systems, which was attributed to reduced oxygen solubility, elevated solution viscosity, and decreased electrode wettability. Electrochemical characterization revealed that the HOPG basal plane exhibited a stable capacitance of ~3.5 μF cm^{-2} at the potential of zero charge, with stronger potassium ion adsorption than fluoride ion adsorption at high electrolyte concentrations. The redox behavior of $K_3Fe(CN)_6$ in the system showed enhanced reversibility at high KF concentrations, and the concentrated electrolyte effectively suppressed HOPG surface passivation caused by airborne/waterborne hydrocarbon adsorption. When applied to symmetric supercapacitors using activated carbon and graphene as active materials, the 17 M KF electrolyte enabled a stable 2.0 V operating voltage, delivering gravimetric capacitances of 221 F g^{-1} (activated carbon) and 56 F g^{-1} (graphene), alongside excellent cycling stability over 10,000 cycles, demonstrating the strong potential of concentrated KF electrolytes for practical energy storage applications. Together, these studies further reinforce the effectiveness of highly concentrated, fluorine-free potassium-based electrolytes in simultaneously widening the electrochemical stability window and maintaining practical ion transport, thereby expanding their applicability in both battery and supercapacitor systems.

In addition to using exclusively fluoride-free anions, employing a dual-anion combination (comprising trace amounts of fluorinated anions and a large proportion of non-fluorinated anions) can significantly enhance the battery's ESW while reducing costs. This study reports a cost-effective, high-performance water-in-bisalt electrolyte for AKIBs by strategically incorporating fluorine-free, low-cost potassium acetate. By pairing a high proportion of hydrophilic OAc^- with a minor fraction of hydrophobic OTf^-, a 36 m eutectic electrolyte ($KOAc_{0.9}OTf_{0.1}\cdot 1.5H_2O$) was formulated. The abundant, inexpensive OAc^- anions establish strong hydrogen bonds with water to maximize salt solubility and eradicate free water molecules. This bi-anion synergy mitigates the severe viscosity and conductivity penalties typical of conventional highly concentrated systems , enabling a high ionic conductivity of 18 mS cm^{-1} and an expanded electrochemical stability window exceeding 4.74 V. This framework offers a practical paradigm for developing sustainable, economically viable high-voltage aqueous batteries. (in Figure 5c)[63]

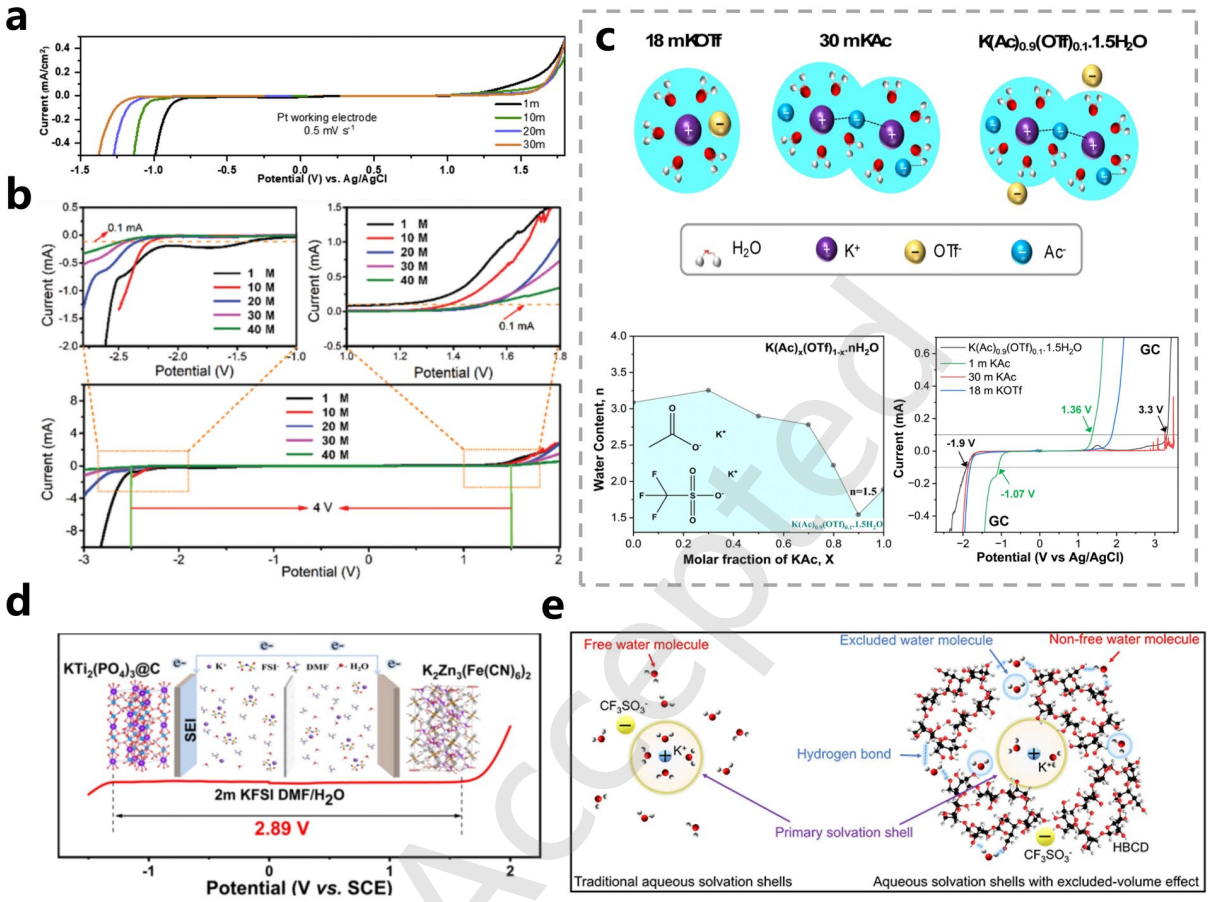

Figure 5. (a) Linear sweep voltammetry curve recorded at 0.5 mV s^{-1} of three-electrode glass cells using Pt as working electrodes, Pt/Ti as counter electrode, Ag/AgCl as reference electrode and the various KOAc electrolytes; (b) Electrochemical stable windows of the HCOOK electrolytes estimated using linear sweep voltammetry at a scan rate of 10 mV s^{-1} with a threshold current of 0.1 mA that is used to determine the onset potentials of water decomposition. (c) Illustration of K^+ solvation in WiSE (KOAc and KOTf) and the eutectic WIBS, liquidus phase diagram at 25°C and the linear sweep voltammetry (LSV) profiles recorded at a scan rate of 1 mV s^{-1} for the solutions $K(Ac)_{0.9}$ $(OTf)_{0.1}\cdot 1.5H_2O$, 1 m KOAc, 30 m KOAc, and 18 m KOTf using a glassy carbon (GC) electrode; (d) Schematic working mechanism of a conventional full AKIB employing a 2 m KFSI–DMF/H_2O hybrid electrolyte, with $KTi_2(PO_4)_3$@C as the anode and $K_2Zn_3(Fe(CN)_6)_2$ as the cathode. (e) Schematic illustration of K^+ solvation shells in a traditional aqueous electrolyte and in the HBCD excluded-volume electrolyte, corresponding to a related aqueous potassium full-cell system (CuHCF||p-PTCDI-EDA) designed to demonstrate wide-voltage and long-cycle potassium storage. Reproduced with permission from Ref. [34] © 2020 Elsevier B.V.; Ref. [61] © The Royal Society of Chemistry 2019; Ref. [63] © 2025 The Royal Society of Chemistry; Ref. [64] © 2021 American Chemical Society; Ref. [65] © 2023 Elsevier B.V.

2.3 Less-Salt Concepts: Supramolecular and Hybrid Coordination

While WIS electrolytes represent a milestone in extending the stability window of aqueous electrolytes, their practical application is constrained by high-salt consumption and cost. These limitations have motivated the

development of less-salt concepts that achieve similar interfacial regulation through supramolecular interactions and hybrid coordination.

Although anion asymmetry offers an elegant route to maintain fluidic superconcentrated regimes , the high-salt cost remains a barrier for grid storage. To break this "concentration dogma," recent strategies shift from multiplying salt molality to designing low-concentration organic/aqueous hybrid electrolytes that manipulate both bulk solvation and interfacial chemistry. This study developed a series of low-concentration N,N-dimethylformamide/water (DMF/H_2O) hybrid electrolytes compatible with lithium, sodium, and potassium salts, which combined a wide electrochemical stable window (2.89 V for 2 m KFSI-based system) with nonflammability, low viscosity (2.8 mPa s^{-1}) and high ionic conductivity (25.3 mS cm^{-1}). (in Figure 5d)[64] Density functional theory calculations revealed that the lower LUMO energy of DMF relative to H_2O drove preferential reduction of DMF and promoted the degradation of FSI^-, enabling the formation of a stable solid electrolyte interphase composed of -CF_x groups and KF on anode surfaces. This interface effectively suppressed the hydrogen evolution reaction, allowing the NASICON-type $KTi_2(PO_4)_3$ @C anode, which was inactive in conventional aqueous electrolytes to deliver a reversible capacity of 76 mAh g^{-1} after 200 cycles at 1 A g^{-1}. When paired with a $K_2Zn_3(Fe(CN)_6)_2$ cathode, the full aqueous potassium-ion battery achieved exceptional rate performance (33 mAh g^{-1} at 20 A g^{-1}) and ultra-long cycling stability over 10 000 cycles, demonstrating the feasibility of low-concentration hybrid electrolytes for safe, durable grid-scale energy storage.

Wei et al. developed a wide-voltage-window amphiphilic supramolecule excluded-volume electrolyte for ultra-durable full-cell aqueous potassium-ion batteries.(in Figure 5e)[65] They introduced low-cost, water-soluble (2-hydroxypropyl)-β-cyclodextrin into 2.0 M KCF_3SO_3 aqueous electrolyte, where the synergistic effect of the excluded-volume effect and hydrogen-bond networks significantly reduced water activity, inhibited active material dissolution, and expanded the electrochemical stability window to over 3.4 V. They paired π-conjugated perylenemide derivative anodes with a copper hexacyanoferrate cathode to assemble full cells, which delivered an open-circuit voltage of 2.0 V, good rate capability up to 30 C, and stable operation across a wide temperature range from -20 to 90 °C. The CuHCF||p-PTCDI-EDA full cell retained 97.8% of its capacity after 10,000 cycles at 10 C, representing an ultralong cycling life among aqueous potassium-ion batteries. This work demonstrated that amphiphilic supramolecule modified excluded-volume electrolytes enabled wide voltage windows, high stability, and temperature tolerance in aqueous batteries for safe, low-cost energy storage.

While macroscopic supramolecular confinement via host-guest exclusion successfully immobilizes active water, optimizing bulk transport kinetics has further inspired the use of tailored small-molecule co-solvents. Rather than utilizing bulky supramolecular hosts, recent strategies employ aprotic organic molecules to reconstruct the precise core-shell solvation sheath of K^+, achieving similar low-salt water suppression with enhanced cost-efficiency. Specifically, this work demonstrated a low-concentration aqueous potassium-ion hybrid electrolyte with a regulated core-shell-solvation structure, achieved by introducing the aprotic additive trimethyl phosphate to suppress water activity.[66] With a salt concentration as low as 1.6 mol L^{-1} potassium trifluoromethanesulfonate, the

electrolyte delivered a widened electrochemical stability window of 3.4 V and inherent non-flammability. Symmetric supercapacitors assembled with this optimized electrolyte operated stably within a 0-2.4 V window and maintained robust performance across a broad temperature range from -20 to 60 °C. Furthermore, a full aqueous potassium-ion battery pairing a Prussian blue analogue cathode with a 3,4,9,10-perylenetetracarboxylic diimide anode achieved a high energy density of 66.5 Wh kg^{-1} at 0.2 C, alongside excellent cycling durability with 84.5% capacity retention after 600 cycles at 0.8 C. This strategy offered a cost-effective route to safe, high-performance aqueous energy storage systems, with the electrolyte cost estimated to be ~50% lower than that of conventional commercial organic potassium-ion electrolytes.

Using a Fe-doped manganese hexacyanoferrate (FeMnHCF-C) cathode, an organic poly(naphthalene-4-formyl-ethylenediamine) (PNFE) anode, and an affordable mixed 2.5 M $Ca(NO_3)_2$ + 1.5 M KNO_3 (CKN2515) electrolyte, the Streng group synergistically enhanced the cycle life of the Mn-based Prussian blue analog cathode through Fe doping, citrate-assisted controlled crystallization, and Ca^{2+} electrolyte additive introduction.[67] The optimized FeMnHCF-C delivered a specific capacity of ~109 mAh g^{-1} with excellent rate capability, while the PNFE anode achieved ~150 mAh g^{-1}. The assembled full cell exhibited a reversible specific capacity of ~60 mAh g^{-1}, an energy density exceeding 70 Wh kg^{-1}, a maximum power density of ~5000 W kg^{-1}, and 80% capacity retention after 600 cycles. Collectively, these strategies highlight that beyond simple salt concentration effects, molecular-level engineering of solvation structures through supramolecular confinement, or organic co-solvent incorporation, offering a powerful route to simultaneously suppress water activity and extend the electrochemical stability window in AKIBs. Besides a high energy density, the full cell delivers a specific capacity of approximately 60 mA h g^{-1}, a power density of 5000 W kg^{-1}, and 80% capacity retention after 600 cycles.

3 Hydrogen-Bond/ Hydration Engineering

As a fundamental non-covalent interaction between a hydrogen atom covalently bonded to an electronegative atom and a neighboring electronegative atom (e.g., an oxygen atom), the hydrogen bond (H-bond) dynamically cross-links in aqueous electrolytes to construct a massive three-dimensional network, which governs the baseline thermodynamic activity of water molecules. In the realm of AKIBs, the localized solvation chemistry of K^+ is synergistically regulated by this short-range electrostatic coordination and the peripheral, long-range hydrogen-bond network.[2, 9, 68-77] Within the immediate primary hydration shell, K^+ is strongly bound to 6–8 water molecules, establishing a formidable kinetic barrier for de-coordination. Concurrently, the extended H-bond network of the bulk phase serves as a structural determinant governing the macro-transport kinetics and interfacial stability. Consequently, rationally restructuring or perturbing this extended O-H···O bonding ecology has emerged as a pivotal strategy in AKIB design. This regulation not only modulates K^+ mobility by altering the water-water clustering status but also profoundly tailors the interfacial desolvation behaviors, thereby fundamentally suppressing parasitic water-induced side reactions and serving as a critical leverage to break through the electrochemical window limitations of aqueous electrolytes (Figure 6). Solvation structure and the hydrogen-bond network describe different but strongly coupled levels of electrolyte organization. The primary K^+ solvation shell is a local, short-range

coordination environment defined by the species directly coordinating K^+. In contrast, the hydrogen-bond network extends through the secondary solvation shell, bulk electrolyte, and interfacial water, and governs the collective connectivity and activity of water molecules. In WiSEs, increasing the salt-to-water ratio first promotes anion entry into the primary K^+ solvation shell and decreases the number of water molecules directly coordinating K^+. The resulting shortage and stronger polarization of water then reduce water contacts, disrupt the extended hydrogen-bond network, and convert free-water clusters into more isolated or strongly bound water states. Therefore, primary-shell reconstruction is the local molecular origin, whereas hydrogen-bond disruption is a coupled higher-level consequence.

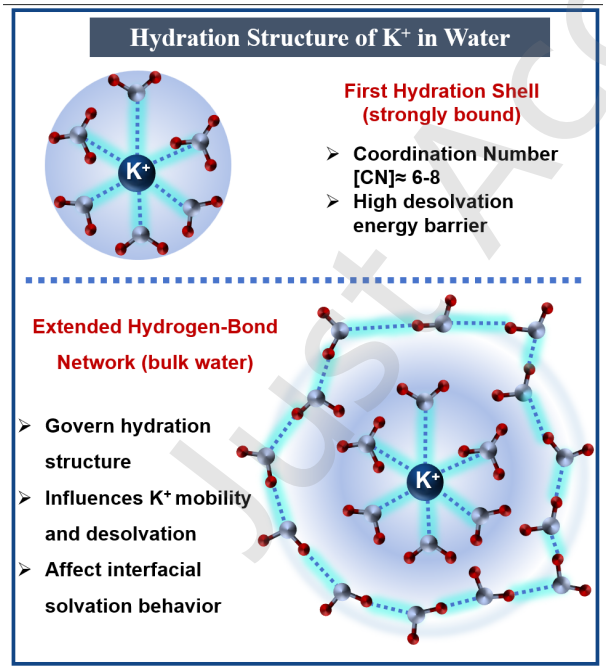

Figure 6. Illustration of Hydrogen-Bond network

3.1 Hydration Engineering for Long Cycling Life

Zhang et al. reported a facile hydration strategy to enhance the air stability and electrochemical performance of P_3-type $K_{0.4}Fe_{0.1}Mn_{0.8}Ti_{0.1}O_2$ by intercalating H_2O molecules into the K-ion layers, which induced a hexagonal-to-monoclinic phase transition and expanded the interlayer spacing to 6.9 Å.[78] The hydrated $K_{0.4}Fe_{0.1}Mn_{0.8}Ti_{0.1}O_2 \cdot 0.16H_2O$ exhibited remarkable tolerance to ambient air for up to 60 days without structural or compositional degradation, suppressed K^+/H^+ exchange, and inhibited Mn^{3+} disproportionation. Benefiting from the "pillar effect" of crystal water and increased pseudocapacitive contribution, the hydrated cathode delivered improved K^+ mobility (lower diffusion barrier of 0.23 eV), less volumetric strain during (de)potassiation, and outstanding rate capability and cycling stability (90% capacity retention after 1000 cycles) in both non-aqueous and aqueous potassium-ion full batteries. This hydration approach was further demonstrated to be applicable to other K-based layered oxides, such as P_3-$K_{0.4}MnO_2$ and P_2-$K_{0.5}Cu_{0.1}Fe_{0.1}Mn_{0.8}O_2$, providing a simple yet effective route to design air-stable, high-performance cathode materials for potassium-ion storage. (in Figure 7a)

While host lattice hydration engineering offers a powerful template for optimizing conventional layered transition metal oxides, expanding the capacity boundaries of aqueous potassium-ion chemistry has also inspired researchers to look beyond single-species intercalation and explore structural frameworks capable of multi-redox reactions. As a prominent alternative to layered pathways, PB analogues present open channels that can be synergistically coupled with hybrid-ion storage mechanism to maximize electrochemical utilization. For instance, Hua et al.(in Figure 7b) developed a novel rechargeable aqueous potassium-hydrogen hybrid ion alkaline battery using potassium nickel hexacyanoferrate ($KNi[Fe(CN)_6]$) as the cathode and nitrogen-doped mesoporous carbon sheets

(NMCSs) as the electrochemical hydrogen storage anode in a concentrated KOH electrolyte.[79] They demonstrated that, unlike in neutral media, both Fe^{2+}/Fe^{3+} redox coupled with K^+ intercalation and $Ni(OH)_2/NiOOH$ redox contributed to the cathode capacity, yielding an ultrahigh specific capacity of 232.7 mAh g^{-1}. The assembled full cell delivered an operating voltage of 1.55 V, a specific capacity of 93.6 mAh g^{-1} at 100 mA g^{-1}, 82.4% capacity retention after 1000 cycles at 2 A g^{-1}, and low self-discharge, suggesting promise for large-scale energy storage applications.

While inorganic open-framework cathodes successfully elevate specific capacity through dual-redox mechanisms, stabilizing the full cell concurrently demands the rational design of high-rate anode platforms. To eliminate dissolution and kinetic barriers, recent engineering has shifted toward conjugated organic molecules optimized with multi-redox-active centers. This study reported a phenazine-derived organic anode, tricyano-substituted hexaazatrinaphthalene (3CN-HATN), for ultrafast and long-life aqueous potassium-ion full cells via targeted molecular engineering.[80] By extending the π-conjugated N-heteroaromatic structure and introducing cyano (C≡N) moieties as additional redox centers, the as-designed 3CN-HATN exhibited a lowered lowest unoccupied molecular orbital energy level favorable for reduction reactions, a narrowed band gap to improve electronic conductivity, and enhanced anti-dissolution performance in aqueous electrolytes. Electrochemical tests demonstrated that the 3CN-HATN anode delivered a remarkable capacity of 233.8 mA h g^{-1} at an ultrahigh rate of 80 C (1 C = 350 mA g^{-1}), while retaining 87.5% of its capacity after cycling at 2 C. When paired with a commercial $Ni(OH)_2$ cathode, the assembled full cell achieved exceptional cycling stability with 81.5% capacity retention after 10,000 cycles at 30 C, outperforming most previously reported aqueous potassium-ion full cells. Mechanistic investigations further confirmed that three C=N and three C≡N moieties in the 3CN-HATN molecule served as multi-redox-active sites for K^+ storage, with a capacitive-dominated charge storage process enabling fast reaction kinetics. This work highlighted the effectiveness of molecular structure modulation in developing high-performance organic electrodes for aqueous potassium-ion batteries.

3.2 Hydrogen-Bond-Regulated and Hydrate-Melt Electrolytes for High-Voltage Potassium-Ion Batteries

Extending from hydration engineering approaches that enhance cycling stability by tailoring ion solvation structures and reducing the activity of free water, recent research has shifted toward more advanced electrolyte designs aimed at simultaneously achieving improved voltage windows and maintaining long-term electrochemical stability. Among these, hydrogen-bond-regulated electrolytes and hydrate melt systems have attracted significant attention, as they offer effective strategies to tune water–ion interactions and enable high-voltage operation in aqueous potassium-ion batteries. A long-lifespan AKIB capable of stable operation at −35 °C was developed, overcoming the low-temperature limitations of conventional AKIBs, which typically operate only above −20 °C and exhibit cycle lives of fewer than 300 cycles under subzero conditions..[81] The researchers designed a 10 m potassium trifluoroacetate (CF_3COOK) electrolyte, whose ultra-low freezing point (-35.5 °C) originated from a high hydrogen-bond breakage degree and elevated average ice formation energy, outperforming traditional KCF_3SO_3-based electrolytes. They paired this electrolyte with a low-solubility Fe-based

Prussian blue analogue cathode ($K_{1.55}Fe[Fe(CN)_6]_{0.95}\cdot 1.03H_2O$) and a commercial 3,4,9,10-perylenetetracarboxylic diimide anode, both of which exhibited high K-storage reversibility in the electrolyte as confirmed by ex situ Fourier transform infrared spectroscopy. The assembled full cell delivered high energy densities of 56.3 Wh kg^{-1} at 25 °C and 41.9 Wh kg^{-1} at -35 °C, alongside exceptional low-temperature cycling stability with 87.5% capacity retention over 1000 cycles at -35 °C, marking a milestone for the application of AKIBs in cold-climate scenarios. (In Figure 7c)

Here, Wang et al. proposed a novel organic/water hybrid electrolyte for AKIBs, using acetamide as a co-solvent and KOTf as the salt.[82] For the first time, this acetamide/water hybrid system was constructed to address the narrow electrochemical stability window bottleneck of conventional aqueous K^+ electrolytes. Benefiting from the strong hydrogen-bonding interactions between acetamide and water, combined with the salt-in-effect of KOTf, the optimized electrolyte achieved an ultralow H_2O / K^+ molar ratio of 1.34, where most water molecules were coordinated into the K^+ solvation shell, effectively suppressing water activity and expanding the ESW to 2.95 V. The hybrid electrolyte also exhibited excellent compatibility with both the organic 3,4,9,10-perylene tetracarboxylic diimide anode and the Ce-doped MnO_2 (Ce-MnO_2) cathode. The assembled Ce-MnO_2||PTCDI full cell delivered a specific capacity of 51.5 mAh g^{-1}, outstanding rate capability, and decent long-term cycling stability with 80.4% capacity retention after 2000 cycles, providing a new electrolyte design paradigm for high-performance AKIBs.

In addition to mitigating low-temperature crystallization via tailored anion speciation, another profound direction within hydrogen-bond regulation relies on formulating organic/aqueous hybrid coordination spheres to concurrently suppress water volatility and maximize anodic oxidation resistance. By substituting free water clustering with robust solvent-acceptor networks, recent milestones have achieved unprecedented high-voltage stability while preserving rapid transport kinetics. This study developed a hydrogen-bond-regulated organic/aqueous hybrid electrolyte (5.6 m KFSI-SCN-H_2O) to address the long-standing narrow electrochemical stability window challenge of AKIBs.[83] SCN acted as a hydrogen bond acceptor to disrupt the strong H_2O-H_2O hydrogen-bond network, converting free H_2O into SCN-restricted immobilized H_2O, which effectively suppressed H_2O activity. Meanwhile, SCN participated in the primary solvation shell of K^+, facilitating the formation of a bilayer cathode electrolyte interphase composed of an SCN-derived outer layer and a KF-rich inner layer. The optimized electrolyte delivered an expanded electrochemical stability window exceeding 4.0 V, with a record-high anodic limit above 5.1 V among reported aqueous K^+ electrolytes, alongside non-flammability, high ionic conductivity, and wide temperature tolerance. The assembled $KVPO_4F$||PTCDI full cell achieved an ultra-long cycle life of 10,000 cycles with a low capacity decay rate of 0.0025% per cycle, and delivered a competitive energy density of ~100 Wh kg^{-1}, representing the highest value among existing AKIB systems. This work provided a novel hydrogen-bond regulation strategy for developing high-energy-density, safe aqueous batteries, and offered theoretical and experimental references for the design of advanced hybrid electrolytes.

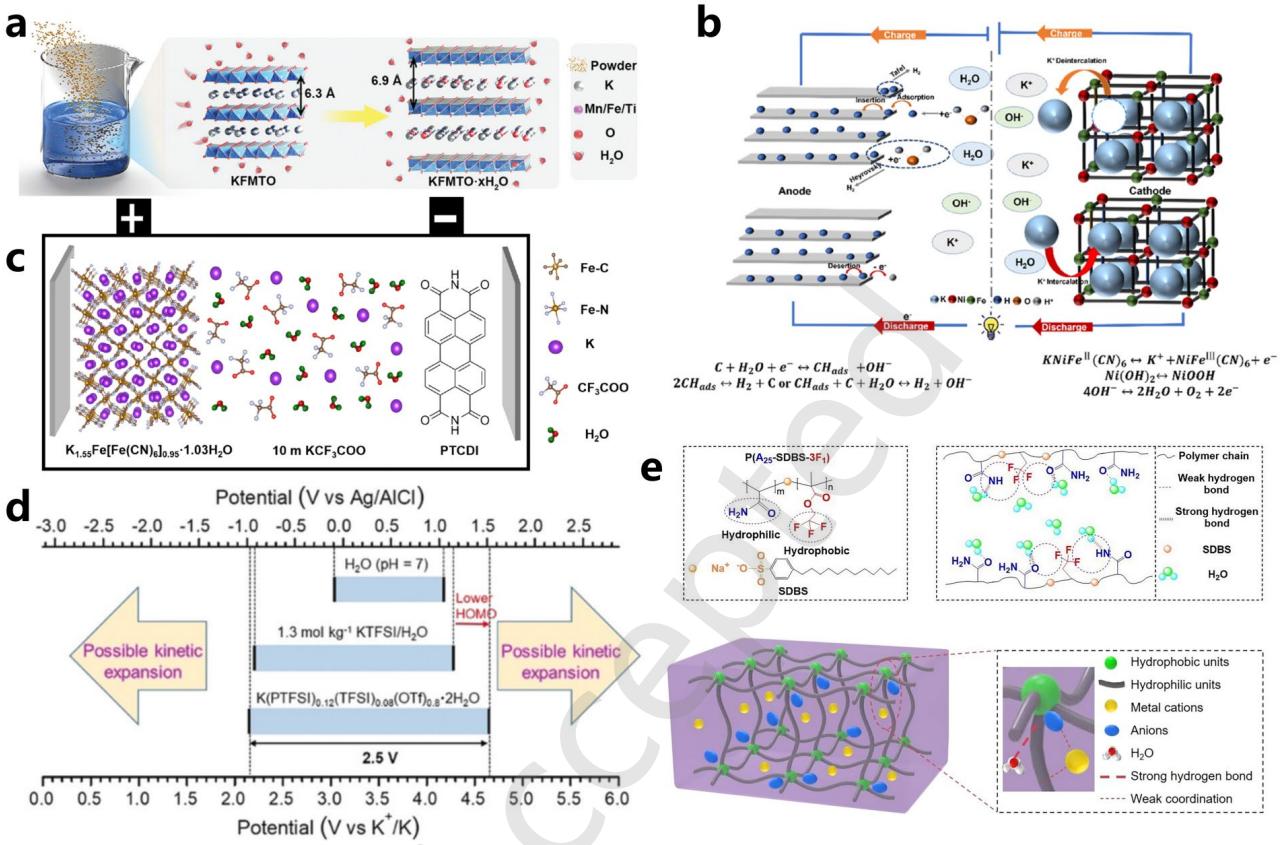

Figure 7. (a) Schematics of the hydration process for KFMTO·xH$_2$O material; (b) Schematic illustration of the KNi[Fe(CN)$_6$](K$^+$)−NMCSs(H$^+$) hybrid ion battery; (c) Working condition of AKIB; (d) Comparison of the potential windows of pure water, 1.3 m KTFSI/H$_2$O solution, and the K(PTFSI)$_{0.12}$-(TFSI)$_{0.08}$(OTf)$_{0.8}$·2H$_2$O hydrate melt. For the K hydrate melt, the anodic limit is extended up to 4.65 V (vs. K$^+$/K at Pt) owing to the lowered HOMO level of the water molecules (red arrow). (e) Structure schematic of hydrophobic-unit-regulated hydrogel electrolytes and schematic diagram of hydrophobicity tuning water molecules in P(A25-SDBS-3F1) hydrogel; The mechanism of hydrophobic-unit regulation in hydrogel electrolytes is shown. Reproduced with permission from Ref. [78] © 2022 Wiley-VCH GmbH; Ref. [79] © 2024 American Chemical Society; Ref. [81] © 2024 American Chemical Society; Ref. [84] © 2019 Wiley-VCH Verlag GmbH & Co. KGaA, Weinheim; Ref.[52] © 2025 Elsevier Inc.

Zheng et al. pioneered the discovery of room-temperature sodium- and potassium-hydrate melts by leveraging asymmetric imide anions with high water solubility and stable chemical structures skipping vulnerable S-F bonds and optimizing ternary eutectic salt systems.[84] Raman spectroscopy and divide-and-conquer density-functional tight-binding molecular dynamics simulations confirmed that nearly all water molecules in these melts were coordinated to alkali metal cations with negligible hydrogen bonding, a structural feature that thermodynamically suppressed water oxidation by lowering the highest occupied molecular orbital level of water. Correspondingly, the electrochemical potential windows were

extended to 2.7 V (vs. Na^+/Na, at Pt) and 2.5 V (vs. K^+/K, at Pt) for the sodium- and potassium-based melts respectively, far exceeding those of conventional dilute aqueous electrolytes. A proof-of-concept aqueous Na-ion full cell pairing a high-voltage $Na_3V_2(PO_4)_2F_3$ cathode with a $NaTi_2(PO_4)_3$ anode delivered a record-high average discharge voltage of 1.75 V and an energy density of 77.9 Wh kg^{-1} based on total electrode mass, demonstrating the feasibility of high-voltage, safe aqueous batteries enabled by these novel hydrate melt electrolytes. (in Figure 7d)

The remarkable widening of stability windows in complex, structurally tailored asymmetric imide melts underscores the critical role of primary solvation shell reconstruction. To systematically trace how simpler, economically viable inorganic alternatives perturb water coordination and dielectric behavior at the nanoscale, recent efforts have shifted toward foundational molecular dynamics simulations, establishing a predictable bridge between concentration-driven clustering and macroscopic transport metrics. Specifically, this study employed molecular dynamics simulations with the OPLS-AA force field and SPC/E water model to systematically investigate the structural, dynamic, and dielectric properties of aqueous potassium fluoride systems across concentrations ranging from 0.1 to 1.0 mol kg^{-1}.[85] The simulations revealed well-defined hydration shells for both K^+ and F^-, with coordination numbers increasing nearly linearly from 6.602 to 6.735 for K^+ and 6.329 to 6.360 for F^- as concentration rose, alongside the identification of contact ion pairs, solvent-separated ion pairs, and double solvent-separated ion pairs via radial distribution function analysis. Concentration-dependent reductions in self-diffusion coefficients were observed, with more pronounced declines for water molecules than for ions, while the dielectric constant decreased from 70.28 to 60.04 with increasing KF content, aligning closely with experimental references. These findings provided critical insights into the concentration-driven modulation of ion-solvent interactions, hydrogen bond network disruption, and transport behaviors in KF electrolytes, offering valuable theoretical support for the design and optimization of potassium-ion battery systems and related electrochemical devices.

3.3 Hydrophobic-Unit-Regulated Hydrogel electrolytes for High Stability

Building on the advances in concentrated and hybrid aqueous electrolytes, recent efforts have increasingly focused on hydrogel architectures with engineered hydrophobic domains, where interfacial water dynamics and ion transport pathways can be precisely regulated to further enhance electrochemical stability and cycling durability in aqueous energy storage systems. Li et al. (Joule, 2025) developed a series of hydrophobic-unit-regulated hydrogel electrolytes (HHEs) by incorporating trace hydrophobic moieties into hydrophilic polymer chains, which delivered a wide electrochemical stability window of 3.3 V even at a high water content of 68 wt% while weakening confinement toward metal cations to boost ion mobility.[52] For potassium aqueous batteries specifically, the optimized HHE enabled a device pairing PTCDI anode and KFeMnHCF cathode to achieve a 1.75 V discharge plateau, a specific capacity exceeding 85 mAh g^{-1}, and a Coulombic efficiency approaching ~99% over 1000 cycles, demonstrating the broad adaptability of the HHE design to diverse aqueous battery systems. (in Figure 7e)

The work from the Dhasarathaboopathy et al. developed a novel eutectic water-in-bisalt (WIBS) electrolyte for potassium-ion batteries via a binary salt strategy combining hydrophilic KOAc and hydrophobic potassium KOTf.[63] The mixed-

anion $K(Ac)_{0.9}(OTf)_{0.1}\cdot 1.5H_2O$ water-in-bisalt electrolyte also perturbs the bulk hydrogen-bond network through cooperative hydrophilic/hydrophobic anion effects. Because its primary design variable is the eutectic salt/water ratio, its formulation, transport properties, and electrochemical performance are discussed in Section 2.2.

Furthermore, research from the Ignaszak group systematically evaluated the chemical compatibility of key components in highly alkaline hydrogel electrolytes for aqueous batteries.[86] Experimental results demonstrated that although acrylamide is a widely adopted monomer in previous formulations, underwent hydrolysis to ammonia and further radical-induced degradation in 6.0 M KOH environments, necessitating its exclusion from alkaline systems. Glycerol, a common cryoprotectant was found to suffer from base-initiated oligomerization to polyglycerols at high loadings, with a maximum feasible addition of 1vol% to maintain hydrogel formation. This optimized formulation retained stable mechanical properties at -80°C, which exhibited ionic conductivities of 46.48 mS/cm at 22°C and 8.67 mS/cm at-23°C respectively, with negligible variation in ion transport parameters (diffusion coefficient ~10^{-8} cm^2/s, ionic mobility ~10^{-7} cm^2/Vs, charge density ~10^{31} cm^{-3}) across temperatures. These results are used here only to emphasize that polymer and cosolvent stability must be verified under the actual pH and temperature of the target electrolyte.

While evaluating chemical compatibility under harsh alkaline conditions ensures hydrogel durability, stabilizing water networks in less corrosive media has inspired alternative matrix designs. To expand the voltage window without relying on extreme concentration penalties, recent strategies shift toward supramolecular engineering to precisely lock water molecules within hydrophilic networks. The Li group developed supramolecular hydrogel electrolytes that expanded the electrochemical stability window without relying on highly concentrated salts.[87] By introducing hydrophilic and superhydrophilic polymer units, they significantly increased the proportion of nonfreezable bound water while suppressing free water content, thereby reducing water activity and mitigating parasitic hydrogen evolution. The optimized hydrogels delivered an electrochemical stability window of up to 3.25 V with high ionic conductivity and low salt concentration. When applied in AKIBs, the electrolyte enabled a high discharge plateau of 1.9V and stable cycling over 3000 cycles, demonstrating an effective strategy for breaking the conventional dependence on ultra-high salt concentrations through supramolecular hydration engineering.

Beyond liquid electrolyte engineering, incorporating water molecules into polymer networks offers an alternative route to modulate water activity and interfacial chemistry. Here, a perspective systematically elucidated the fundamental mechanisms of dendrite suppression in aqueous batteries enabled by hydrogels.[88] It first established the theoretical linkage between dendrite formation and key parameters including exchange current density, limiting current density, and sand time, then clarified the regulatory roles of hydrogel components: polymer networks were shown to modulate water activity by tuning the proportion of free, intermediate, and bound water, while solute and cosolvent introduction further optimized the thermodynamic environment to suppress hydrogen evolution side reactions. The work also demonstrated that hydrogels regulated ion solvation structures, enhanced cation transport numbers via single-ion conduction designs and promoted progressive nucleation modes to guide uniform zinc deposition.

Although this study focuses on zinc-ion batteries based on aqueous systems, its findings also provide valuable guidance for the design of AKIBs with gel electrolytes. Additionally, it revealed the synergistic effect of hydrogel mechanical modulus and interfacial compatibility on dendrite inhibition, providing a theoretical foundation for the rational design of high-stability hydrogel electrolytes for aqueous energy storage systems.

4 Cross-Strategy Comparison and Interfacial Chemistry

The electrolyte strategies discussed above regulate aqueous potassium-ion storage through different but closely coupled mechanisms, including concentration-driven solvation reconstruction, hydrogen-bond regulation, and polymer-mediated water confinement. However, the reported electrochemical stability window (ESW) alone cannot provide a complete comparison because the practical stability of an aqueous electrolyte also depends on ionic transport, electrode chemistry, current-collector stability, testing protocol, and interfacial passivation. Likewise, reported full-cell energy densities may differ substantially depending on the cell configuration and mass basis used for calculation. Therefore, Table 1 provides a protocol-aware comparison of representative electrolyte systems in terms of electrolyte composition, transport properties, ESW measurement conditions, full-cell performance, energy density, and practical limitations.

Table 1 Representative electrolytes and device specifications. (m: mol kg^{-1} solvent, M: mol L^{-1} solution)

Reference	Electrolyte and concentration basis	Transport property	ESW and protocol	Cell operating voltage	Energy density	Advantages	Limitations and cost/sustainability caveat
[31]	22 M KOTf	76 mS cm^{-1} at 25 °C; 10 mS cm^{-1} at −20 °C	≈3.0 V; LSV on Ti mesh, 10 mV s^{-1}	KFeMnHCF-3565//PTCDI; 0–2.6 V	80 Wh kg^{-1}; total active mass of cathode + anode	High conductivity; broad temperature range; validated pouch cell	Very high salt loading; fluorinated anion; viscosity, recovery, and salt cost require system-level assessment
[17]	$K(FSI)_{0.6}(OTf)_{0.4}\cdot H_2O$	-	2.56 V; Al cathodic-limit and Pt anodic-limit scans; ±5 μA cm^{-2} threshold	PBA//PTCDI AKIB	-	Suppresses PTCDI dissolution; KF-containing SEI; stabilizes PBA morphology	Fluorinated salts; near-stoichiometric water; viscosity and interphase-growth kinetics need quantification
[35]	30 m KFSI	24 mS cm^{-1} reported in a later comparative study	3.97 V; linear voltammetry, 10 mV s^{-1}	KFHCF//β-PTCDA	41 Wh kg^{-1}	Suppresses organic-electrode dissolution and HER; good rate capability	High FSI salt loading and fluorine burden; energy-density basis must be explicit
[59]	20 m KOTf + 30 m KFSI in a hydrogel	4.34 mS cm^{-1}	3.02 V; Ti//Ti two-electrode LSV, 10 mV s^{-1}	KMnFe(CN)6//KTi2(PO4)3@C; reported 2.8 V operation	-	Leakage suppression; mechanical integrity; long cycling	Extremely high salt and fluorine content; lower conductivity than liquid electrolytes; polymer recovery not assessed
[34]	20 m KOAc + 2 wt% CMC	-	LSV with Pt working electrode, Pt/Ti counter electrode, Ag/AgCl reference, 0.5 mV s^{-1}	KMHCF-based electrode demonstration	-	Fluorine-free; reduced water mobility and Fe/Mn leaching	Strong alkalinity can cause Al pitting and transition-metal dissolution; 'low cost' is salt-material level only
[61]	40 m HCOOK; H_2O:salt ≈1.38:1	46 mS cm^{-1}	≈4.0 V (−2.5 to 1.5 V vs Ag/AgCl); glassy carbon; 10 mV s^{-1}; 0.1 mA threshold	Related supercapacitor and KTP electrode tests; not a conventional AKIB full cell	-	Fluorine-free; high conductivity; wide apparent window	Very high salt loading; electrode-dependent ESW; alkaline corrosion; no full-cell AKIB energy density
[63]	$K(Ac)_{0.9}(OTf)_{0.1}\cdot 1.5H_2O$; reported apparent K^+ concentration 36.1 M	18.07 mS cm^{-1} at 25 °C	>4.74 V; LSV at 1 mV s^{-1}; GC and separate Al/Ti limit tests	AKIB full-cell configuration should be stated from original source	-	Fluorine-reduced mixed-anion design; high conductivity relative to viscosity	Still high salt loading and 10 mol% OTf; apparent ESW depends strongly on electrode and threshold
[64]	2 m KFSI in DMF/H_2O	25.3 mS cm^{-1}; viscosity 2.8 mPa s	2.89 V	$K_2Zn_3[Fe(CN)_6]_2$//$KTi_2(PO_4)_3$@C AKIB	-	Low salt; good conductivity; SEI formation enables KTP anode	DMF toxicity and recovery; still uses fluorinated KFSI; nonflammability does not establish complete safety
[65]	2.0 M KOTf + (2-hydroxypropyl)-β-cyclodextrin	-	>3.4 V	CuHCF//p-PTCDI-EDA; OCV ≈2.0 V	-	Low salt; 10,000-cycle durability; wide temperature range	Additive cost, viscosity, biodegradability, and recovery require evaluation

Reference	Electrolyte and concentration basis	Transport property	ESW and protocol	Cell operating voltage	Energy density	Advantages	Limitations and cost/sustainability caveat
[66]	1.6 M KOTf + trimethyl phosphate	-	3.4 V	PBA//PTCDI AKIB	66.5 Wh kg^{-1}	Low salt; broad temperature range; potentially lower salt cost	Organic cosolvent toxicity/volatility and recyclability; source mass basis and electrolyte amount required
[81]	10 m CF_3COOK	-	-	Fe-PBA//PTCDI AKIB	56.3 Wh kg^{-1} at 25 °C; 41.9 Wh kg^{-1} at −35 °C	Exceptional low-temperature cycling	High salt loading; fluorinated carboxylate; low-temperature viscosity and electrolyte-to-capacity ratio should be reported
[83]	5.6 m KFSI–SCN–H_2O	-	>4.0 V; anodic limit >5.1 V	$KVPO_4F$//PTCDI AKIB	≈100 Wh kg^{-1}	High voltage	KFSI and succinonitrile content; toxicity, recovery, and protocol-dependent anodic limit require caution
[52]	HHE with 68 wt% water and low salt content	-	3.3 V	KFeMnHCF//PTCDI; discharge plateau ≈1.75 V	-	High water content; leakage control; weak cation confinement and good cycling	Polymer/additive synthesis and recovery; interphase composition and growth kinetics remain unresolved

As summarized in Table 1, fluorinated WiSEs and hydrate melts remain highly effective for reducing free-water activity and enabling high-voltage operation, but they generally require high salt loadings and may suffer from increased viscosity, fluorinated-salt consumption, and limited low-temperature fluidity. Fluorine-free acetate- and formate-based electrolytes reduce dependence on fluorinated salts and can maintain favorable ionic transport, although their alkaline environments may introduce current-collector corrosion and transition-metal dissolution.[34] By contrast, hybrid, supramolecular, and hydrogel electrolytes increasingly shift the design principle from simply increasing salt concentration toward regulating local coordination, hydrogen bonding, and interfacial water accessibility.[64, 65] These comparisons also indicate that terms such as "fluorine-free," "low-salt," or "nonflammable" should not be directly equated with low cost, environmental friendliness, or complete safety. Salt consumption, cosolvent toxicity and volatility, corrosion, recyclability, electrolyte recovery, and gas evolution should also be considered, while quantitative sustainability claims ultimately require dedicated techno-economic and life-cycle assessments.

Macroscopic performance, however, does not fully explain why different electrolytes can operate beyond the thermodynamic stability window of water. The practical ESW is jointly controlled by bulk water activity and interfacial processes, including water accessibility, charge-transfer kinetics, and electrolyte-derived passivation. An apparently wide ESW may therefore originate from thermodynamic suppression of water activity, kinetic restriction of water at the electrode surface, preferential electrolyte decomposition to form a protective interphase, or a combination of these effects. Table 2 consequently compares representative electrolyte classes from an interfacial perspective, including their dominant solvation regulation, available evidence for interphase formation, passivation effects, and major limitations.

Table 2 Interfacial Engineering and Chemistry of Representative AKIB Electrolytes

Electrolyte	Dominant solvation regulation	Growth kinetics and direct evidence	Passivation effect	Principal limitation
Fluorinated WiSE	Anion-rich primary solvation; strongly reduced free-water population	SECM maps slow apparent electron transfer; OEMS resolves H_2 onset. Passivation near −1.3 V vs Ag/AgCl but remains spatially heterogeneous	Delays HER; suppresses organic-electrode dissolution; enables low-potential redox	May renew HER below −1.4 V nearly, high salt/viscosity
Fluorine-free acetate/formate WiSE	High cation/anion coordination and reduced solvent power; often alkaline	Mainly ex situ XPS, SEM/EDS, separator analysis, and corrosion observations	Reduces dissolution and water accessibility; gelation can reduce leaching	Al pitting, high-pH Fe/Mn dissolution, incomplete electronic passivation
LiFSI/LiOTf hydrate melt	Near-stoichiometric hydration; negligible uncoordinated water	Interphase composition inferred from ex situ characterization	PTCDI insolubility; reduced morphology and crystal degradation of PBA	High viscosity; expensive fluorinated salts; uncertain long-term interphase renewal
Hydrogen bond -regulated organic/aqueous hybrid	Cosolvent competes for Hydrogen bonds and can enter the K^+ solvation shell	Spectroscopy, electrochemistry, calculations, and selected ex situ interphase analysis	Suppresses HER/OER and dissolution at lower salt concentration	Cosolvent decomposition, toxicity/volatility, and composition drift
Hydrophobic/supramolecular hydrogel	Water confinement, hydrophobic domains, bound-water enrichment, and mechanical contact	Mostly indirect water-state spectroscopy, electrochemistry, and mechanical tests	Suppresses leakage and local water access, may reduce dissolution and stabilize contact	Polymer degradation, interfacial delamination, transport heterogeneity, unknown film renewal

Among the electrolyte classes summarized in Table 2, fluorinated WiSEs currently provide the most direct evidence for interphase-mediated passivation. In highly concentrated $K(FSI)_{0.6}(OTf)_{0.4}$ electrolyte, scanning electrochemical microscopy (SECM) revealed a decrease in the apparent electron-transfer rate around −1.3 V versus Ag/AgCl, consistent with formation of a passivating interphase, while operando electrochemical mass spectrometry (OEMS) showed that detectable H_2 evolution was shifted from approximately −0.9 V in dilute electrolyte to potentials below approximately −1.4 V.[89] Importantly, the SECM response remained spatially heterogeneous and H_2 evolution re-emerged at more negative potentials, demonstrating that the WiSE-derived interphase delays rather than completely eliminates HER. In hydrate-melt electrolytes, fluorinated-anion decomposition has similarly been associated with KF-containing interphases and suppression of PTCDI dissolution, although the time-dependent growth, thickness, and spatial uniformity of these interphases remain much less directly resolved.[90]

Fluorine-free and hydrogen-bond-regulated systems exhibit somewhat different interfacial behavior. In concentrated KOAc electrolytes, improved stability is mainly associated with reduced water activity, decreased solvent power, and concentration-dependent stabilization of electrode and current-collector surfaces. Nevertheless, strongly alkaline conditions can promote Al pitting and Fe/Mn dissolution, demonstrating that suppression of water activity does not automatically ensure complete interfacial stability.[83] The dominant interfacial challenges also differ between individual cell components. At negative electrodes, HER, active-material dissolution, and incomplete interphase coverage are the major failure modes. An effective negative-electrode interphase must therefore suppress electronic transfer to water

while maintaining sufficient K^+ conductivity. At positive electrodes, OER, electrolyte oxidation, transition-metal dissolution, and host-structure degradation become more important, requiring a thin but protective cathode–electrolyte interphase that limits direct contact with reactive water. Current collectors constitute an additional component of the practical stability window: concentrated KOAc systems, for example, demonstrate that an apparently stable electrolyte may still cause localized Al corrosion under strongly alkaline conditions.[83] Consequently, ESWs measured on glassy carbon, Pt, Al, or Ti should not be regarded as directly interchangeable without considering the corresponding interfacial and corrosion behavior.

Finally, the level of mechanistic evidence remains uneven among different electrolyte classes. Ex situ XPS, SEM/EDS, Raman spectroscopy, and simulations provide valuable information on interphase composition and solvation structure, but they cannot directly resolve the formation kinetics and spatial evolution of interfacial layers. SECM and OEMS provide complementary information on local electronic passivation and real-time gas evolution, respectively, while cryogenic transmission electron microscopy (Cryo-TEM) and cryogenic surface spectroscopy offer promising approaches for preserving and resolving highly hydrated and metastable interphases.[91] At present, systematic operando and cryogenic comparisons among fluorinated WiSEs, fluorine-free WiSEs, hydrate melts, hybrid electrolytes, and hydrophobic hydrogels remain limited. Future studies combining SECM/OEMS with operando spectroscopy and Cryo-TEM should therefore focus on the composition, thickness, spatial coverage, growth, rupture, and renewal of interphases under realistic polarization conditions. Future research should reduce reliance on high loadings of fluorinated imide salts where this can be achieved without compromising transport, interfacial stability, or low-temperature operation. Fluorine-free or fluorine-reduced formulations may decrease the raw-material contribution of the electrolyte, while organic cosolvents should be selected with explicit consideration of toxicity, volatility, recovery, and recyclability. Their system-level economic and environmental advantages must be verified through dedicated techno-economic and life-cycle assessments rather than inferred solely from salt identity or nonflammability.

Conclusion & Outlook

In summary, expanding the ESW of aqueous electrolytes represents the most critical path to breaking through the energy density bottleneck of AKIBs, which typically falls below 80 Wh kg^{-1} due to parasitic water splitting.[38, 92-94] To bypass the thermodynamic 1.23 V limit of dilute solutions , the research paradigm has symmetrically evolved into two primary electrolyte engineering pillars: the WIS strategy, which locks the vast majority of water molecules within a dense primary K^+ solvation sheath to eliminate uncoordinated free water and promote passivating interphases.[71] And the "hydrogen-bond regulation" strategy, which introduces polar co-solvents, supramolecular hosts, or hydrogel matrices to disrupt the bulk water hydrogen-bonding network and deactivate free water at lower salt costs. These methodologies have undergone significant technological shifts from early fluorinated superconcentrated regimes to cost-effective, eco-friendly fluorine-free alternatives (such as KOAc and KF) , and have ultimately culminated in "less-salt" concepts that leverage minimal active components for micro-scale confinement. Collectively, these advancements provide dual thermodynamic and kinetic leverage to pave a solid foundation for secure, high-voltage, and high-energy-density

aqueous potassium-based energy storage.[95, 96]

To transition these laboratory breakthroughs into viable grid-scale energy storage, future research must first overcome the concentration-viscosity dilemma, decoupling wide potential windows from the economic and low-temperature penalties of extreme concentration. Blindly pursuing ultra-high salt concentrations introduces severe practical drawbacks, including exorbitant costs of fluorinated salts, increased electrolyte viscosity, diminished ionic conductivity, and a propensity for salt precipitation under cold-climate conditions.[97, 98] Future electrolyte designs must break this "concentration dogma" through molecular-level coordination engineering. On one hand, emphasis should be placed on utilizing advanced asymmetric imide anions that exhibit highly localized coordination and lowered lattice energy to foster contact-ion-pair aggregates , or leveraging binary/ternary eutectic hydrate melts to preserve excellent low-temperature transport kinetics and fluidity over broad temperature ranges[99]. On the other hand, for hydrogel architectures, precise regulation of hydrophobic-to-hydrophilic phase separation—by incorporating trace hydrophobic moieties into hydrophilic polymer networks—can firmly confine active water molecules within local domains, simultaneously boosting metal cation mobility via weakened confinement to harmonize wide voltage windows with superionic transport behaviors.[83, 100]

Secondly, decoding the transient and complex interfacial chemistry to mitigate severe electrode degradation must be prioritized as an indispensable directive. Under high-voltage operation, the macro-scale structural durability of electrode materials is fundamentally governed by the performance of the interface of electrolyte and electrode. Currently, water-derived interphases often exhibit heterogeneous surface coverage, failing to completely suppress hydrogen evolution at extreme negative potentials or prevent current collector pitting and transition metal (Fe/Mn/V) dissolution.[93] Resolving these challenges necessitates the standardized deployment of multi-scale operando characterizations coupled with advanced computational methods. Operando scanning electrochemical microscopy[101] should be routinely applied to map localized electron transfer rates and the onset potentials of water splitting at the interface , paired with operando electrochemical mass spectrometry[102] for the real-time, highly sensitive quantification of gaseous byproducts (H_2 and O_2). Furthermore, cryogenic transmission electron microscopy (Cryo-TEM)[103] is urgently required to resolve the atomic-scale crystalline or amorphous configurations of KF-rich or organic-rich passivating layers. These empirical insights must be seamlessly integrated with machine learning force field (MLFF) molecular dynamics simulations to accurately reconstruct the dynamic behavior of the electric double layer (EDL) under extreme polarization, thereby providing deterministic guidance for the rational design of dense, electronically insulating, and ion-permeable corrosion-resistant interfaces. [104-110]

Finally, validating realistic full-cell metrics under commercially relevant conditions is the ultimate prerequisite for accelerating the industrial deployment of AKIBs. Academic evaluations must resolutely transition from flooded, three-electrode configurations or half-cells with excessive counter-electrodes toward realistic pouch cells featuring lean electrolyte conditions and high mass-loading electrodes.[39, 111] Within this practical assessment framework, monitoring the internal gas pressure evolution during long-term cycling is mandatory, requiring the engineering of sophisticated safety valves or chemical scavengers to handle gas generation.

Concurrently, given the high mass-loading constraints, the synergistic effect of the hydrogel mechanical modulus and interfacial compatibility on dendrite inhibition must be thoroughly explored to guide uniform progressive nucleation and suppress localized short circuits. Most critically, comprehensive techno-economic analyses (TEA) and life-cycle cost (LCC) evaluations must be integrated into the electrolyte design process from the outset.[112-116]Research must completely decouple its reliance from prohibitively expensive and environmentally hazardous fluorinated imide salts. Instead, by harmonizing affordable inorganic salts (such as acetates) with eco-friendly organic co-solvents to construct low-cost hybrid configurations, the total manufacturing cost can be driven significantly below that of conventional nonaqueous systems, thereby fundamentally reshaping the commercial landscape of safe, sustainable, and grid-scale energy storage.

Declaration of competing interest

The authors declare that they have no known competing financial interests or personal relationships that could have appeared to influence the work reported in this paper.

Acknowledgments

This work was financially supported by the Beijing Natural Science Foundation (No. Z220020), the National Natural Science Foundation of China (NSFC) Young Scientists Fund (Category A) (22525504) and Postdoctoral Fellowship Program of CPSF (GZC20250052).

References

[1] Hou, W.-h.; Lu, Y.; Ou, Y.; Zhou, P.; Yan, S.; He, X.; Geng, X.; Liu, K. Recent Advances in Electrolytes for High-Voltage Cathodes of Lithium-Ion Batteries. *Transactions of Tianjin University* **2023**, *29* (2), 120–135.
[2] Li, C.; Goh, S.; Ou, Y.; Sun, C.; Yan, S.; Hou, W.; Lu, Y.; Ma, X.; Liu, Z.; Wu, Y.; et al. Supramolecular self-assembly in solid-state lithium batteries: Bulk electrolyte design and interface engineering. *Supramolecular Materials* **2025**, *4*.
[3] Liu, Z.; Lu, Y.; Ma, X.; He, Y.; Fu, M.; Yan, S.; Li, C.; Song, X.; Zhou, H.; Liu, K. Advanced Functional Optical Fiber Sensors for Smart Battery Monitoring. *Energy Material Advances* **2024**, *5*.
[4] Lu, Y.; Cao, Q.; Zhang, W.; Zeng, T.; Ou, Y.; Yan, S.; Liu, H.; Song, X.; Zhou, H.; Hou, W.; et al. Breaking the molecular symmetricity of sulfonimide anions for high-performance lithium metal batteries under extreme cycling conditions. *Nature Energy* **2024**.
[5] Lu, Y.; Zhang, W.; Liu, S.; Cao, Q.; Yan, S.; Liu, H.; Hou, W.; Zhou, P.; Song, X.; Ou, Y.; et al. Tuning the Li+ Solvation Structure by a "Bulky Coordinating" Strategy Enables Nonflammable Electrolyte for Ultrahigh Voltage Lithium Metal Batteries. *ACS Nano* **2023**, *17* (10), 9586–9599.
[6] Xia, Y.; Zhou, P.; Kong, X.; Tian, J.; Zhang, W.; Yan, S.; Hou, W.-h.; Zhou, H.-Y.; Dong, H.; Chen, X.; et al. Designing an asymmetric ether-like lithium salt to enable fast-cycling high-energy lithium metal batteries. *Nature Energy* **2023**, *8* (9), 934–945.
[7] Yan, S.; Liu, F.; Ou, Y.; Zhou, H.-Y.; Lu, Y.; Hou, W.; Cao, Q.; Liu, H.; Zhou, P.; Liu, K. Asymmetric Trihalogenated Aromatic Lithium Salt Induced Lithium Halide Rich Interface for Stable Cycling of All-Solid-State Lithium Batteries. *ACS Nano* **2023**, *17* (19), 19398–19409.
[8] Yan, S.; Lu, Y.; Liu, F.; Xia, Y.; Li, Q.; Liu, K. Zwitterionic Matrix with Highly Delocalized Anionic Structure as an Efficient Lithium Ion Conductor. *CCS Chemistry* **2023**, *5* (7), 1612–1622.
[9] Yan, S.; Wang, Z.; Liu, F.; Zhou, H.; Liu, K. Aromatic Donor–Acceptor Charge-Transfer Interactions Reinforced Supramolecular Polymer Electrolyte for Solid-State Lithium Batteries. *Advanced Functional Materials* **2023**, *33* (52).
[10] Zhou, H. Y.; Ou, Y.; Yan, S. S.; Xie, J.; Zhou, P.; Wan, L.; Xu, Z. A.; Liu, F. X.; Zhang, W. L.; Xia, Y. C.; et al. Supramolecular Polymer Ion Conductor with Weakened Li Ion Solvation Enables Room Temperature All-Solid-State

Lithium Metal Batteries. *Angewandte Chemie International Edition* **2023**, *62* (35).
[11] Zhou, P.; Hou, W.; Xia, Y.; Ou, Y.; Zhou, H.-Y.; Zhang, W.; Lu, Y.; Song, X.; Liu, F.; Cao, Q.; et al. Tuning and Balancing the Donor Number of Lithium Salts and Solvents for High-Performance Li Metal Anode. *ACS Nano* **2023**, *17* (17), 17169–17179.
[12] Hou, W.-h.; Ou, Y.; Zeng, T.; Feng, Q.; Cao, Q.; Zhou, P.; Xia, Y.; Song, X.; Zhang, W.; Lu, Y.; et al. Rational molecular design of electrolyte additive endows stable cycling performance of cobalt-free 5 V-class lithium metal batteries. *Energy & Environmental Science* **2024**, *17* (21), 8325–8336.
[13] Ou, Y.; Li, C.; Zhou, H.; Zhou, P.; Yan, S.; Hou, W.; Lu, Y.; Ma, X.; Wu, Y.; Wu, S.; et al. Supramolecular Chemistry for High-Performance Lithium Metal Batteries. *CCS Chemistry* **2025**, *7* (10), 2864–2898.
[14] Kim, K.; Ma, H.; Park, S.; Choi, N.-S. Electrolyte-Additive-Driven Interfacial Engineering for High-Capacity Electrodes in Lithium-Ion Batteries: Promise and Challenges. *ACS Energy Letters* **2020**, *5* (5), 1537–1553.
[15] Nguyen, M. T.; Pham, H. Q.; Berrocal, J. A.; Gunkel, I.; Steiner, U. An electrolyte additive for the improved high voltage performance of LiNi(0.5)Mn(1.5)O(4) (LNMO) cathodes in Li-ion batteries. *J Mater Chem A Mater* **2023**, *11* (14), 7670–7678. From NLM PubMed-not-MEDLINE.
[16] Aurbach, D.; Markevich, E.; Salitra, G. High Energy Density Rechargeable Batteries Based on Li Metal Anodes. The Role of Unique Surface Chemistry Developed in Solutions Containing Fluorinated Organic Co-solvents. *Journal of the American Chemical Society* **2021**, *143* (50), 21161–21176.
[17] Hosaka, T.; Noda, A.; Kubota, K.; Chiguchi, K.; Matsuda, Y.; Ida, K.; Yasuno, S.; Komaba, S. Superconcentrated NaFSA–KFSA Aqueous Electrolytes for 2 V-Class Dual-Ion Batteries. *ACS applied materials & interfaces* **2022**, *14* (20), 23507–23517.
[18] Lu, Y.; Yan, S.; He, Y.; Liu, Z.; Ma, X.; Ou, Y.; Zhang, W.; Liu, K. Understanding and tuning intermolecular interactions of the electrolyte solvation structure for low-temperature lithium-based batteries. *Energy Storage Materials* **2024**, *72*.
[19] Ma, X.; Lu, Y.; Ou, Y.; Yan, S.; Hou, W.; Zhou, P.; Liu, K. Strategies for flame-retardant polymer electrolytes for safe lithium-based batteries. *Nano Research* **2024**, *17* (10), 8754–8771.
[20] Ou, Y.; Zhou, P.; Hou, W.; Ma, X.; Song, X.; Yan, S.; Lu, Y.; Liu, K. Smart materials for safe lithium-ion batteries against thermal runaway. *Journal of Energy Chemistry* **2024**, *94*, 360–392.
[21] Xia, Y.; Hou, W.; Zhou, P.; Ou, Y.; Cheng, G.; Guo, C.; Liu, F.; Zhang, W.; Yan, S.; Lu, Y.; et al. Trace Dual-Salt Electrolyte Additive Enabling a LiF-Rich Solid Electrolyte Interphase for High-Performance Lithium Metal Batteries. *Nano Letters* **2024**.
[22] Yan, S.; Liu, H.; Chen, X.; Lu, Y.; Cao, Q.; Liu, K. Ionic solid-like conductor-assisted polymer electrolytes for solid-state lithium metal batteries. *Science China Chemistry* **2024**, *67* (12), 4116–4124.
[23] Zhang, W.; Lu, Y.; Cao, Q.; Liu, H.; Feng, Q.; Zhou, P.; Xia, Y.; Hou, W.; Yan, S.; Liu, K. A reversible self-assembled molecular layer for lithium metal batteries with high energy/power densities at ultra-low temperatures. *Energy & Environmental Science* **2024**, *17* (13), 4531–4543.
[24] Zhou, P.; Ou, Y.; Feng, Q.; Xia, Y.; Zhou, H.; Hou, W. h.; Song, X.; Lu, Y.; Yan, S.; Zhang, W.; et al. Tuning the Nucleophilicity of Anion in Lithium Salt to Enable an Anion-Rich Solvation Sheath for Stable Lithium Metal Batteries. *Advanced Functional Materials* **2024**, *35* (10).
[25] Zhou, P.; Xiang, Y.; Liu, K. Understanding and applying the donor number of electrolytes in lithium metal batteries. *Energy & Environmental Science* **2024**, *17* (21), 8057–8077.
[26] Wessells, C. D.; Huggins, R. A.; Cui, Y. Copper hexacyanoferrate battery electrodes with long cycle life and high power. *Nature Communications* **2011**, *2* (1).
[27] Ji, B.; Zhang, F.; Song, X.; Tang, Y. A Novel Potassium-Ion-Based Dual-Ion Battery. *Advanced Materials* **2017**, *29* (19).
[28] Liu, Y.; Tai, Z.; Zhang, Q.; Wang, H.; Pang, W. K.; Liu, H. K.; Konstantinov, K.; Guo, Z. A new energy storage system: Rechargeable potassium-selenium battery. *Nano Energy* **2017**,

35, 36–43.
[29] Zou, X.; Xiong, P.; Zhao, J.; Hu, J.; Liu, Z.; Xu, Y. Recent research progress in non-aqueous potassium-ion batteries. *Phys. Chem. Chem. Phys.* **2017**, *19* (39), 26495–26506.
[30] Ren, W.; Chen, X.; Zhao, C. Ultrafast Aqueous Potassium-Ion Batteries Cathode for Stable Intermittent Grid-Scale Energy Storage. *Advanced Energy Materials* **2018**, *8* (24).
[31] Jiang, L.; Lu, Y.; Zhao, C.; Liu, L.; Zhang, J.; Zhang, Q.; Shen, X.; Zhao, J.; Yu, X.; Li, H.; et al. Building aqueous K-ion batteries for energy storage. *Nature Energy* **2019**, *4* (6), 495–503.
[32] Suo, L.; Borodin, O.; Gao, T.; Olguin, M.; Ho, J.; Fan, X.; Luo, C.; Wang, C.; Xu, K. "Water-in-salt" electrolyte enables high-voltage aqueous lithium-ion chemistries. *Science* **2015**, *350* (6263), 938–943.
[33] Li, P.; Zheng, X.; Yu, H.; Zhao, G.; Shu, J.; Xu, X.; Sun, W.; Dou, S. X. Electrochemical potassium/lithium-ion intercalation into TiSe2: Kinetics and mechanism. *Energy Storage Materials* **2019**, *16*, 512–518.
[34] Han, J.; Mariani, A.; Zhang, H.; Zarrabeitia, M.; Gao, X.; Carvalho, D. V.; Varzi, A.; Passerini, S. Gelified acetate-based water-in-salt electrolyte stabilizing hexacyanoferrate cathode for aqueous potassium-ion batteries. *Energy Storage Materials* **2020**, *30*, 196–205.
[35] Chen, H.; Zhang, Z.; Wei, Z.; Chen, G.; Yang, X.; Wang, C.; Du, F. Use of a water-in-salt electrolyte to avoid organic material dissolution and enhance the kinetics of aqueous potassium ion batteries. *Sustainable Energy & Fuels* **2020**, *4* (1), 128–131.
[36] Neff, V. D. Electrochemical oxidation and reduction of thin films of Prussian blue. *Journal of the Electrochemical Society* **1978**, *125* (6), 886–887.
[37] Li, L.; Hu, Z.; Lu, Y.; Wang, C.; Zhang, Q.; Zhao, S.; Peng, J.; Zhang, K.; Chou, S. L.; Chen, J. A Low-Strain Potassium-Rich Prussian Blue Analogue Cathode for High Power Potassium-Ion Batteries. *Angewandte Chemie International Edition* **2021**, *60* (23), 13050–13056.
[38] Shu, W.; Li, J.; Zhang, G.; Meng, J.; Wang, X.; Mai, L. Progress on Transition Metal Ions Dissolution Suppression Strategies in Prussian Blue Analogs for Aqueous Sodium-/Potassium-Ion Batteries. *Nano-Micro Letters* **2024**, *16* (1).
[39] Xu, C.; Yang, Z.; Zhang, X.; Xia, M.; Yan, H.; Li, J.; Yu, H.; Zhang, L.; Shu, J. Prussian Blue Analogues in Aqueous Batteries and Desalination Batteries. *Nano-Micro Letters* **2021**, *13* (1).
[40] 王 Wang, 洁.; 邢 Xing, 超.; 杨 Yang, 荞.; 戚 Qi, 海.; 周 Zhou, 小. 锰基普鲁士蓝作为钠/钾离子电池正极的研究进展. *Chinese Science Bulletin 科学通报* **2025**, *71*, 2064–2080.
[41] Zhou, C.; Yuan, Z.; Hu, Z.; Wu, Y.; Duan, L.; Du, Y.; Zhou, X. Energy storage mechanisms and optimization strategies of polymer cathodes for potassium-ion batteries. *Acta Physico-Chimica Sinica* **2026**, 100363.
[42] Yuan, Z.; Chen, L.; Liao, J.; Song, L.; Chen, A.; Yan, D.; Wang, J.; Zhou, X. Methyl Asymmetric Interference-Enhanced Dipole–Dipole Interaction for High-Performance Potassium–Graphite Battery Electrolyte Design. *Angewandte Chemie International Edition* **2026**, *65* (12), e23473.
[43] Li, R.; Du, Y.; Lei, Y.; Song, L.; Sun, J.; Man, Y.; Wang, G.; Zhou, X. High-Performance, Activation-Free Magnesium-Ion Batteries Enabled by Ionic Liquid Electrolyte Additive. *Angewandte Chemie International Edition* **2026**, *65* (34), e7580996.
[44] Song, L.; Tan, M.; Zhang, S.; Tang, H.; Qi, H.; Yuan, Z.; Sun, L.; Zhou, X.; Guo, Z. Rational Construction and Modulation of Built-In Electric Field for High-Efficiency Alkali Metal-Based Batteries. *Angewandte Chemie International Edition* **2026**, *65* (16), e6795880.
[45] Qi, H.; Du, Y.; Ding, J.; Song, L.; Liao, J.; Yu, C.; Yuan, Z.; Chen, S.; Zhou, X. Regulating interface electric field to stabilize high-voltage KVPO4F positive electrode for sustainable potassium-ion batteries. *Nature Communications* **2026**, *17* (1), 4943.
[46] Dong, Q.; Yao, X.; Zhao, Y.; Qi, M.; Zhang, X.; Sun, H.; He, Y.; Wang, D. Cathodically stable Li-O2 battery operations using water-in-salt electrolyte. *Chem* **2018**, *4* (6), 1345–1358.
[47] Hosaka, T.; Kubota, K.; Hameed, A. S.; Komaba, S. Research development on K-ion batteries. *Chemical reviews* **2020**, *120* (14), 6358–6466.
[48] Fan, L.; Chen, S.; Ma, R.; Wang, J.; Wang,

L.; Zhang, Q.; Zhang, E.; Liu, Z.; Lu, B. Ultrastable potassium storage performance realized by highly effective solid electrolyte interphase layer. *Small* **2018**, *14* (30), 1801806.
[49] Hosaka, T.; Takahashi, R.; Kubota, K.; Tatara, R.; Matsuda, Y.; Ida, K.; Kuba, K.; Komaba, S. Origin of enhanced capacity retention of aqueous potassium-ion batteries using monohydrate-melt electrolyte. *Journal of Power Sources* **2022**, *548*.
[50] Vardhini, G.; Dilip, P. S.; Kumar, S. A.; Suriyakumar, S.; Hariharan, M.; Shaijumon, M. M. Polyimide-Based Aqueous Potassium Energy Storage Systems Using Concentrated WiSE Electrolyte. *ACS Applied Materials & Interfaces* **2024**, *16* (37), 48782–48791.
[51] Liu, T.; Liu, K.-T.; Wang, J.; Ji, X.; Lan, P.; Mu, Z.; Pan, Y.; Cheng, S.; Liu, M. Achievement of a polymer-free KAc gel electrolyte for advanced aqueous K-Ion battery. *Energy Storage Materials* **2021**, *41*, 133–140.
[52] Li, C.; Wang, T.; Lai, H. C. J.; Park, S. W.; Chan, W. Y. K.; Li, Q.; Zhao, Y.; Fan, J.; Pei, Z.; Zhi, C. Hydrophobic-unit-regulated hydrogel electrolytes with high water content and low salt concentration for high-voltage aqueous batteries. *Joule* **2025**, *9* (4).
[53] Xia, M.; Zhou, J.; Lu, B. Comprehensive Insights into Aqueous Potassium-Ion Batteries. *Advanced Energy Materials* **2024**, *15* (12).
[54] Niu, X.; Wang, L.; Chen, Y.; Li, H.; Hou, G.; Lu, J.; Bai, Y.; Zhang, S.; Xing, Y.; Fedotov, S. S.; et al. Electrolyte and Electrode Design for Aqueous Potassium-Ion Batteries. *ChemSusChem* **2026**, *19* (8).
[55] Leonard, D. P.; Wei, Z.; Chen, G.; Du, F.; Ji, X. Water-in-Salt Electrolyte for Potassium-Ion Batteries. *ACS Energy Letters* **2018**, *3* (2), 373–374.
[56] Amiri, M.; Béguin, F.; Bélanger, D. Electrochemical Charge Storage Properties of Porous Carbon Electrodes in Salt-in-Water and Water-in-Salt Potassium Acetate Electrolytes. *Electrochimica Acta* **2026**, 148539.
[57] Wessells, C. D.; Peddada, S. V.; Huggins, R. A.; Cui, Y. Nickel Hexacyanoferrate Nanoparticle Electrodes For Aqueous Sodium and Potassium Ion Batteries. *Nano Letters* **2011**, *11* (12), 5421–5425.
[58] Liang, G.; Gan, Z.; Wang, X.; Jin, X.; Xiong, B.; Zhang, X.; Chen, S.; Wang, Y.; He, H.; Zhi, C. Reconstructing vanadium oxide with anisotropic pathways for a durable and fast aqueous K-ion battery. *ACS nano* **2021**, *15* (11), 17717–17728.
[59] Li, Y.; Zhou, Z.; Deng, W.; Li, C.; Yuan, X.; Hu, J.; Zhang, M.; Chen, H.; Li, R. A Superconcentrated Water-in-Salt Hydrogel Electrolyte for High-Voltage Aqueous Potassium-Ion Batteries. *ChemElectroChem* **2021**, *8* (8), 1451–1454.
[60] Kumaresan, T. K.; Ikhe, A. B.; Park, W. B.; Prabakar, S. R.; Noh, H. S.; Seo, J. Y.; Lee, Y. K.; Sohn, K. S.; Kwak, J. S.; Pyo, M. Highly Concentrated Asymmetric KTFSI for Aqueous Potassium Ion Batteries. *Advanced Energy Materials* **2024**, *14* (38), 2402011.
[61] Liu, T.; Tang, L.; Luo, H.; Cheng, S.; Liu, M. A promising water-in-salt electrolyte for aqueous based electrochemical energy storage cells with a wide potential window: highly concentrated HCOOK. *Chemical Communications* **2019**, *55* (85), 12817–12820.
[62] Iamprasertkun, P.; Ejigu, A.; Dryfe, R. A. Understanding the electrochemistry of "water-in-salt" electrolytes: basal plane highly ordered pyrolytic graphite as a model system. *Chemical science* **2020**, *11* (27), 6978–6989.
[63] Dhasarathaboopathy, M.; Sabhapathy, P.; Gurkan, B. Water-in-bisalt electrolytes with mixed hydrophilic and hydrophobic anions for enhanced transport and stability for potassium-ion batteries. *RSC advances* **2025**, *15* (1), 94–100.
[64] Yuan, X.; Li, Y.; Zhu, Y.; Deng, W.; Li, C.; Zhou, Z.; Hu, J.; Zhang, M.; Chen, H.; Li, R. Low Concentration DMF/H2O Hybrid Electrolyte: A New Opportunity for Anode Materials in Aqueous Potassium-Ion Batteries. *ACS Applied Materials & Interfaces* **2021**, *13* (32), 38248–38255.
[65] Wei, J.; Zhang, P.; Liu, Y.; Zhu, M.; Dai, T.; Tie, Z.; Jin, Z. Wide-voltage-window amphiphilic supramolecule excluded-volume electrolytes for ultra-durable full-cell aqueous potassium-Ion batteries. *Chemical Engineering Journal* **2023**, *459*, 141623.
[66] Chen, J.; Lei, S.; Zhang, S.; Zhu, C.; Liu, Q.; Wang, C.; Zhang, Z.; Wang, S.; Shi, Y.; Yin, L.; et al. Dilute Aqueous Hybrid Electrolyte with

Regulated Core-Shell-Solvation Structure Endows Safe and Low-Cost Potassium-Ion Energy Storage Devices. *Advanced Functional Materials* **2023**, *33* (19).
[67] Streng, R. L.; Steeger, T.; Senyshyn, A.; Abel, S.; Schneider, P.; Benning, C.; Naranjo, B. M.; Gryc, D.; Hussain, M. Z.; Lieleg, O. A low-cost and high-energy aqueous potassium-ion battery. *Journal of Energy Chemistry* **2025**, *106*, 523–531.
[68] Chen, T.; Qin, B.; Liu, Y.; Jin, Z.; Wu, H.; Wang, C.; Zhang, X. A Fluorinated, Ion-Conducting and Adaptive Supramolecular Polymer Protective Layer for Stabilizing Lithium Metal Anodes. *CCS Chemistry* **2024**, *6* (5), 1157–1164.
[69] Cheng, X. B.; Zhang, R.; Zhao, C. Z.; Zhang, Q. Toward Safe Lithium Metal Anode in Rechargeable Batteries: A Review. *CHEMICAL REVIEWS* **2017**, *117* (15), 10403–10473.
[70] Yang, L. L.; Tan, X. X.; Wang, Z. Q.; Zhang, X. Supramolecular Polymers: Historical Development, Preparation, Characterization, and Functions. *CHEMICAL REVIEWS* **2015**, *115* (15), 7196–7239.
[71] Lu, Z. Y.; Guo, Y.; Zhang, S. W.; Wu, S. C.; Meng, R. W.; Hong, S.; Li, J. X.; Xue, H. Y.; Zhang, B. Y.; Fan, D. H.; et al. Crowning Metal Ions by Supramolecularization as a General Remedy toward a Dendrite-Free Alkali-Metal Battery. *ADVANCED MATERIALS* **2021**, *33* (31).
[72] Qin, B.; Yin, Z.; Tang, X.; Zhang, S.; Wu, Y.; Xu, J.-F.; Zhang, X. Supramolecular polymer chemistry: From structural control to functional assembly. *Progress in Polymer Science* **2020**, *100*, 101167.
[73] Guo, P.; Su, A.; Wei, Y.; Liu, X.; Li, Y.; Guo, F.; Li, J.; Hu, Z.; Sun, J. Healable, Highly Conductive, Flexible, and Nonflammable Supramolecular Ionogel Electrolytes for Lithium-Ion Batteries. *ACS Applied Materials & Interfaces* **2019**, *11* (21), 19413–19420.
[74] Fang, X.; Tian, N.; Hu, W.; Qing, Y.; Wang, H.; Gao, X.; Qin, Y.; Sun, J. Dynamically Cross-Linking Soybean Oil and Low-Molecular-Weight Polylactic Acid toward Mechanically Robust, Degradable, and Recyclable Supramolecular Plastics. *Advanced Functional Materials* **2022**, *32* (46), 2208623.
[75] Ma, H.; Xu, W.; Tang, X.; Kang, Y.; Xu, J.-F.; Zhang, X. A Supramolecularly Activatable Photosensitizer: Controllable Cyanine J-Aggregation for Efficient Photodynamic Therapy. *CCS Chemistry* **2025**, *7* (3), 832–842.
[76] Yin, Z.; Yang, Y.; Yang, J.; Song, G.; Hu, H.; Zheng, P.; Xu, J.-F. Supramolecular Polymerization Powered by Escherichia coli: Fabricating a Near-Infrared Photothermal Antibacterial Agent in Situ. *CCS Chemistry* **2022**, *4* (10), 3285–3295.
[77] Lugger, S. J. D.; Houben, S. J. A.; Foelen, Y.; Debije, M. G.; Schenning, A. P. H. J.; Mulder, D. J. Hydrogen-Bonded Supramolecular Liquid Crystal Polymers: Smart Materials with Stimuli-Responsive, Self-Healing, and Recyclable Properties. *Chemical Reviews* **2022**, *122* (5), 4946–4975.
[78] Zhang, X.; Yang, X.; Sun, G.; Yao, S.; Xie, Y.; Zhang, W.; Liu, C.; Wang, X.; Yang, R.; Jin, X. Hydration enables air-stable and high-performance layered cathode materials for both organic and aqueous potassium-ion batteries. *Advanced Functional Materials* **2022**, *32* (41), 2204318.
[79] Hua, R.; Xu, C.; Yang, H.; Qu, D.; Zhang, R.; Liu, D.; Tang, H.; Li, J.; Qu, D. Potassium-Hydrogen Hybrid Ion Alkaline Battery: A New Rechargeable Aqueous Battery Combined a K+ Storage Cathode and an Electrochemical Hydrogen Storage Anode. *Acs Applied Materials & Interfaces* **2024**, *16* (16), 20520–20532.
[80] Zheng, Y.; Yu, D.; Wang, J.; Yang, J.; Luo, W.; Ge, T.; Qin, L.; Huang, Y.; Chen, D. A phenazine-derived organic anode for ultrafast and long-life aqueous potassium-ion full cells. *Science China Materials* **2024**, *67* (5), 1464–1470.
[81] Jiang, L.; Lu, Y.-C. Building a long-lifespan aqueous K-ion battery operating at− 35 C. *ACS Energy Letters* **2024**, *9* (3), 985–991.
[82] Wang, S.; Wang, S.; Chen, L.; Long, L.; Xing, Y.; Deng, L.; Wang, L. Acetamide as the co-solvent for stable aqueous K-ion batteries. *Journal of Power Sources* **2025**, *638*, 236633.
[83] Xia, M.; Fu, H.; Lin, K.; Rao, A. M.; Cha, L.; Liu, H.; Zhou, J.; Wang, C.; Lu, B. Hydrogen-bond regulation in organic/aqueous hybrid electrolyte for safe and high-voltage K-ion batteries. *Energy & Environmental Science* **2024**,

17 (3), 1255–1265.
[84] Zheng, Q.; Miura, S.; Miyazaki, K.; Ko, S.; Watanabe, E.; Okoshi, M.; Chou, C.; Nishimura, Y.; Nakai, H.; Kamiya, T.; et al. Sodium- and Potassium-Hydrate Melts Containing Asymmetric Imide Anions for High-Voltage Aqueous Batteries. *Angewandte Chemie-International Edition* **2019**, *58* (40), 14202–14207.
[85] Lahmidi, A.; Rabii, S.; Errougui, A.; Chtita, S.; El Kouali, M.; Talbi, M. Investigation of structural, dynamic and dielectric properties of an aqueous potassium fluoride system at various concentrations by molecular dynamics simulations. *Journal of the Serbian Chemical Society* **2024**, *89* (6), 877–890.
[86] Khor, C. K.; Blackstone, C. C.; Ignaszak, A. An Insight into Synthesis of the Antifreeze Alkaline Hydrogel Electrolyte: Fine-Tuning Chemistries for Efficient Ion Transport. *ChemElectroChem* **2023**, *10* (16), e202300113.
[87] Li, C.; Zhu, X.; Wang, D.; Yang, S.; Zhang, R.; Li, P.; Fan, J.; Li, H.; Zhi, C. Fine tuning water states in hydrogels for high voltage aqueous batteries. *Acs Nano* **2024**, *18* (4), 3101–3114.
[88] Xian, J.; Fu, R.; Liu, K.; Yang, P. Insights into Dendrite Regulation by Polymer Hydrogels for Aqueous Batteries. *ACS Nano* **2025**, *19* (14), 13491–13504.
[89] Gossage, Z. T.; Ito, N.; Hosaka, T.; Tatara, R.; Komaba, S. In situ Observation of Evolving H2 and Solid Electrolyte Interphase Development at Potassium Insertion Materials within Highly Concentrated Aqueous Electrolytes. *Angewandte Chemie International Edition* **2023**, *62* (43), e202307446.
[90] Hosaka, T.; Takahashi, R.; Kubota, K.; Tatara, R.; Matsuda, Y.; Ida, K.; Kuba, K.; Komaba, S. Origin of enhanced capacity retention of aqueous potassium-ion batteries using monohydrate-melt electrolyte. *Journal of Power Sources* **2022**, *548*, 232096.
[91] Gao, Z.; Yao, J.; Yan, J.; Sun, J.; Du, C.; Dai, Q.; Su, Y.; Zhao, J.; Chen, J.; Li, X.; et al. Atomic-Scale Cryo-TEM Studies of the Electrochemistry of Redox Mediator in Li–O2 Batteries. *Small* **2024**, *20* (30), 2311739.
[92] Chen, Z.; Li, X.; Qiu, C.; Wu, Z.; Deng, J.; Wang, Z.; Wu, L.; Yu, H.; Yan, L.; Zhang, L.; et al. Expanding electrolyte window enables high voltage aqueous batteries: Challenges and strategies. *Energy Storage Materials* **2026**, *84*.
[93] Rynearson, L.; Antolini, C.; Jayawardana, C.; Yeddala, M.; Hayes, D.; Lucht, B. L. Speciation of Transition Metal Dissolution in Electrolyte from Common Cathode Materials. *Angewandte Chemie International Edition* **2023**, *63* (5).
[94] Shimoda, Y.; Matsui, Y.; Tonoya, T.; Ishikawa, M. Potassium Bis(fluorosulfonyl)imide Is an Effective Additive for Improving Anode Cyclability in Sulfolane-Based Electrolytes for Li–S Batteries. *ACS Applied Energy Materials* **2023**, *6* (17), 8909–8918.
[95] Charles, D. S.; Feygenson, M.; Page, K.; Neuefeind, J.; Xu, W.; Teng, X. Structural water engaged disordered vanadium oxide nanosheets for high capacity aqueous potassium-ion storage. *Nature Communications* **2017**, *8* (1).
[96] Di Pietro, M. E.; Mele, A. Deep eutectics and analogues as electrolytes in batteries. *Journal of Molecular Liquids* **2021**, *338*.
[97] Doronin, S. V.; Nazarov, M. A. Superconcentrated Electrolytes for Aqueous Batteries Based on Alkali Metal Formates and Propionates. *The Journal of Physical Chemistry C* **2022**, *126* (34), 14611–14625.
[98] Ilic, S.; Lavan, S. N.; Connell, J. G. Anion-derived contact ion pairing as a unifying principle for electrolyte design. *Chem* **2024**, *10* (10), 2987–3007.
[99] Li, L.; Chen, Y.; Shao, W.; He, Q.; Wahyudi, W.; Kumar, P.; Li, Q.; Zhang, J. Suppressed hydrogen evolution reactions via modulating hydrogen bonds in aqueous battery electrolytes by additives. *Materials Science and Engineering: R: Reports* **2026**, *169*.
[100] Wang, Y.; Tang, F.; Yu, X.; Chiang, K.-Y.; Yu, C.-C.; Ohto, T.; Chen, Y.; Nagata, Y.; Bonn, M. Interfaces govern the structure of angstrom-scale confined water solutions. *Nature Communications* **2025**, *16* (1).
[101] Snook, G. A.; Huynh, T. D.; Hollenkamp, A. F.; Best, A. S. Rapid SECM probing of dissolution of LiCoO2 battery materials in an ionic liquid. *Journal of Electroanalytical Chemistry* **2012**, *687*, 30–34.
[102] Xing, L.-Y.; Yan, C.; Huang, J.-Q.

Decoupling gas evolution in full batteries with dual-DEMS. *Joule* **2026**, *10* (3), 102383.
[103] Gao, Z.; Yao, J.; Yan, J.; Sun, J.; Du, C.; Dai, Q.; Su, Y.; Zhao, J.; Chen, J.; Li, X.; et al. Atomic-Scale Cryo-TEM Studies of the Electrochemistry of Redox Mediator in Li–O2 Batteries. *Small* **2024**, *20* (30).
[104] Shen, Z. H.; Liu, H. X.; Shen, Y.; Hu, J. M.; Chen, L. Q.; Nan, C. W. Machine learning in energy storage materials. *INTERDISCIPLINARY MATERIALS* **2022**, *1* (2), 175–195.
[105] Zhao, J. Y.; Feng, X. N.; Pang, Q. Q.; Fowler, M.; Lian, Y. B.; Ouyang, M. G.; Burke, A. F. Battery safety: Machine learning-based prognostics. *PROGRESS IN ENERGY AND COMBUSTION SCIENCE* **2024**, *102*.
[106] Klemm, C. P.; Frömling, T. Machine-learning based Li-Ion Cell state prediction using Impedance spectroscopy. *MACHINE LEARNING WITH APPLICATIONS* **2025**, *22*.
[107] Zhai, Q. X.; Jiang, H. M.; Long, N. B.; Kang, Q. L.; Meng, X. H.; Zhou, M. J.; Yan, L. J.; Ma, T. L. Machine learning for full lifecycle management of lithium-ion batteries. *RENEWABLE & SUSTAINABLE ENERGY REVIEWS* **2024**, *202*.
[108] Wei, Z.; He, Q.; Zhao, Y. Machine learning for battery research. *JOURNAL OF POWER SOURCES* **2022**, *549*.
[109] Wang, T. T.; Liu, K. Y.; Peng, H. J.; Liu, X. Y. Interpretable Machine Learning for Battery Prognosis: Retrospect and Prospect. *ADVANCED ENERGY MATERIALS* **2025**, *15* (48).
[110] Qiu, Y.; Zhang, X.; Tian, Y.; Zhou, Z. Machine learning promotes the development of all-solid-state batteries. *CHINESE JOURNAL OF STRUCTURAL CHEMISTRY* **2023**, *42* (9).
[111] Yokoyama, Y.; Fukutsuka, T.; Miyazaki, K.; Abe, T. Origin of the Electrochemical Stability of Aqueous Concentrated Electrolyte Solutions. *Journal of The Electrochemical Society* **2018**, *165* (14), A3299–A3303.
[112] Arie, A. A.; Kristianto, H.; Cengiz, E. C.; Demir-Cakan, R. Waste tea-based porous carbon-sulfur composite cathodes for lithium-sulfur battery. *IONICS* **2020**, *26* (1), 201–212.
[113] He, Q. S.; Chen, H. X.; Chen, X.; Zheng, J. J.; Que, L. F.; Yu, F. D.; Zhao, J. H.; Xie, Y. M.; Huang, M. L.; Lu, C. Z.; et al. Tea-Derived Sustainable Materials. *ADVANCED FUNCTIONAL MATERIALS* **2024**, *34* (11).
[114] Guven, D.; Kayalica, M. O. Life-cycle assessment and life-cycle cost assessment of lithium-ion batteries for passenger ferry. *TRANSPORTATION RESEARCH PART D-TRANSPORT AND ENVIRONMENT* **2023**, *115*.
[115] Bahmei, F.; de Buruaga, A. S.; Bautista, S. P.; Olarte, J.; Ajuria, J.; Varzi, A.; Weil, M. Life Cycle Assessment and Life Cycle Costing of Supercapacitors: A Comprehensive Review and Assessment of Environmental and Economic Impacts. *CHEMSUSCHEM* **2025**, *18* (21).
[116] Rapa, M.; Gobbi, L.; Ruggieri, R. Environmental and Economic Sustainability of Electric Vehicles: Life Cycle Assessment and Life Cycle Costing Evaluation of Electricity Sources. *ENERGIES* **2020**, *13* (23).